TreeGen: A Bayesian Generative Model for Hierarchies

Marcel Kollovieh[1,2,3] **Nils Fleischmann**[4] **Filippo Guerranti**[1,2,3]

Bertrand Charpentier[4] **Stephan Günnemann**[1,2,3,4]

[1] School of Computation, Information and Technology, Technical University of Munich
[2] Munich Data Science Institute [3] Munich Center for Machine Learning [4] Pruna AI

Correspondence to: `m.kollovieh@tum.de`

Abstract

In this work, we introduce TreeGen, a novel generative framework modeling distributions over hierarchies. We extend Bayesian Flow Networks (BFNs) to enable transitions between probabilistic and discrete hierarchies parametrized via categorical distributions. Our proposed scheduler provides smooth and consistent entropy decay across varying numbers of categories. We empirically evaluate TreeGen on the jet-clustering task in high-energy physics, demonstrating that it consistently generates valid trees that adhere to physical constraints and closely align with ground-truth log-likelihoods. Finally, by comparing TreeGen's samples to the exact posterior distribution and performing likelihood maximization via rejection sampling, we demonstrate that TreeGen outperforms various baselines.

1 Introduction

Hierarchies are central to representing complex relationships across diverse domains. Consequently, hierarchical clustering algorithms are core components in well-established machine libraries such as scikit-learn [36], and find applications in a wide range of fields, spanning from phylogenetics and particle physics to web and citation network analysis. In phylogenetics, for example, clustering algorithms group organisms or genetic sequences based on similarity, helping to infer evolutionary relationships [18]. Further, real-world systems, from neural representation [22] to citation networks and web graphs [37] often exhibit hierarchical organization. Importantly, in high-energy physics, agglomerative linkage algorithms are indispensable for jet clustering and provide insights into the substructure of particle collisions [7].

Traditional hierarchical clustering algorithms operate primarily in an *unsupervised* setting. *Agglomerative* methods greedily merge clusters with the shortest distance until only a single root remains [21]. *Divisive* algorithms work in a top-down approach and start with all points in a single cluster and iteratively split them into smaller groups [43, 14]. More recent methods optimize global cost functions via continuous relaxations, yet the setting remains unsupervised [11, 34, 9, 48, 30]. This is sensible in many applications, as ground truth hierarchies are often unavailable for supervised training.

Jet clustering in high-energy physics is a prime example where supervised simulations are available, yet traditional algorithms remain unsupervised. In particle accelerators, high-energy collisions produce unstable particles that successively decay and split into more particles. This resulting spray of particles, also known as a *jet*, is detected by particle detectors. The task in jet clustering is to reconstruct the latent hierarchy that describes the splitting process from the observed constituents, i.e., leaves of the hierarchy [33]. Simulators are extensively used in this field to generate collision events based on a physical model, enabling the creation of realistic hierarchy datasets for jet clustering [3, 4, 12]. Yet, despite this availability, prevailing jet-clustering pipelines often still rely on unsupervised algorithms [15, 46, 7, 17].

To address this problem, we introduce a novel generative model for hierarchies. Building on Bayesian Flow Networks (BFNs) [19] and Bayesian Sample Inference (BSI) [31], our model explicitly models the posterior distribution over hierarchies.

Our *key contributions* are summarized as follows:

- **Generative Model for Hierarchies.** We introduce TreeGen, a novel generative model tailored to tree-structured data. The model transitions between probabilistic and discrete hierarchies parametrized via categorical distributions.
- **Entropy Scheduler for BFNs.** We propose an alternative entropy scheduler for BFNs that provides smooth transitions of categorical distributions from uniform to discrete states across varying numbers of categories.
- **Application to Jet Clustering.** We demonstrate the practical effectiveness of our generative model by applying it to the jet clustering task using data from the GINKGO simulator [12].

2 Background

2.1 Probabilistic Hierarchies

Let $\hat{\mathcal{T}}$ be a rooted hierarchy, also called a tree, with n leaves $V = \{\mathrm{v}_1, \ldots, \mathrm{v}_n\}$ and n' internal nodes $Z = \{\mathrm{z}_1, \ldots, \mathrm{z}_{n'}\}$, where $\mathrm{z}_{n'}$ is the root. We represent the hierarchy via two binary adjacency matrices:

$$\hat{\boldsymbol{A}} \in \{0,1\}^{n \times n'}, \quad \hat{\boldsymbol{B}} \in \{0,1\}^{n' \times n'}, \tag{1}$$

where the entry $\hat{\boldsymbol{A}}_{ij}$ encodes an edge from leaf v_i to internal node z_j, and $\hat{\boldsymbol{B}}_{ij}$ encodes an edge from internal node z_i to internal node z_j.

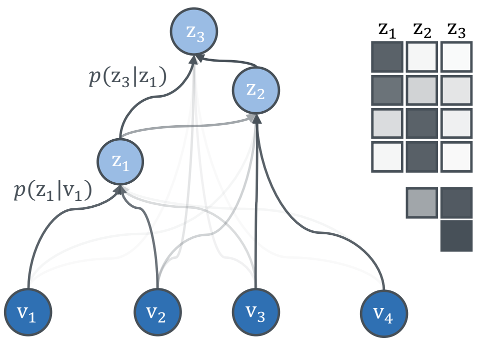

z_1 z_2 z_3
$p(\mathrm{z}_3|\mathrm{z}_1)$
$p(\mathrm{z}_1|\mathrm{v}_1)$
z_3
z_2
z_1
v_1
v_2
v_3
v_4

Figure 1: Example of a probabilistic hierarchy. The matrices represent $\boldsymbol{A}$ and $\boldsymbol{B}$, respectively.

We enforce both matrices to be row-stochastic and additionally constrain $\hat{\boldsymbol{B}}$ to be upper triangular to ensure they define a valid tree-structure. In the binary case, this means that each row contains exactly one non-zero entry, while the last row of $\hat{\boldsymbol{B}}$ is all zeros because the root has no parent. These constraints guarantee that $(\hat{\boldsymbol{A}}, \hat{\boldsymbol{B}})$ encodes a valid rooted tree.

Following Zügner et al. [48], we relax these matrices to *probabilistic* assignments:

$$\boldsymbol{A} \in [0,1]^{n \times n'}, \quad \boldsymbol{B} \in [0,1]^{n' \times n'}, \tag{2}$$

while retaining the row-stochastic and upper-triangular constraints. We interpret each row of $\boldsymbol{A}$ and $\boldsymbol{B}$ as a categorical distribution over parent assignments:

$$\boldsymbol{A}_{ij} = p(\mathrm{z}_j \mid \mathrm{v}_i), \quad \boldsymbol{B}_{ij} = p(\mathrm{z}_j \mid \mathrm{z}_i), \tag{3}$$

denoting the probability that internal node z_j is the parent of leaf v_i and the probability that z_j is the parent of internal node z_i, respectively. Together, the matrices describe a *probabilistic hierarchy* $\mathcal{T} = (\boldsymbol{A}, \boldsymbol{B})$. By interpreting each row of a probabilistic hierarchy as a categorical distribution, we can sample valid discrete hierarchies. An example of a probabilistic hierarchy is shown in Fig. 1.

2.2 Bayesian Flow Networks

Bayesian Flow Networks (BFNs) form a class of generative models that refine a belief over a target sample via successive Bayesian updates [19]. Recently, Lienen et al. [31] proposed Bayesian Sample

Project page: cs.cit.tum.de/daml/treegen

Inference (BSI), including BFNs in a more general framework, which we adopt here for notational simplicity. BSI starts with an initial belief over $\boldsymbol{x} \in \mathbb{R}^D$ using a Gaussian prior with precision λ,

$$p(\boldsymbol{x}) \;=\; \mathcal{N}(\boldsymbol{\mu}, \lambda^{-1}), \quad \boldsymbol{\mu} \in \mathbb{R}^D,\ \lambda > 0, \tag{4}$$

which is updated in a Bayesian manner: $p(\boldsymbol{x} \mid \boldsymbol{y}) \propto p(\boldsymbol{y} \mid \boldsymbol{x})p(\boldsymbol{x})$. At each step, we observe a noisy measurement

$$\boldsymbol{y} \sim \mathcal{N}(\boldsymbol{x}, \alpha^{-1}), \quad \alpha > 0, \tag{5}$$

where α denotes the precision of the measurement. We compute the closed-form Gaussian posterior

$$p(\boldsymbol{x} \mid \boldsymbol{y}) \;=\; \mathcal{N}\Big(\tfrac{\lambda\boldsymbol{\mu}+\alpha\,\boldsymbol{y}}{\lambda+\alpha},\, (\lambda+\alpha)^{-1}\Big), \tag{6}$$

which converges towards the true $\boldsymbol{x}$ as the precision λ increases by α with each update. As we do not have direct access to the sample noisy measurements $\boldsymbol{y}$ of $\boldsymbol{x}$, we train a neural network $\hat{\boldsymbol{x}} = f_{\boldsymbol{\theta}}(\mu, \lambda)$ to approximate $\boldsymbol{x}$. The model is trained similarly to diffusion models [23] and minimizes the squared error between $\hat{\boldsymbol{x}}$ and the ground truth $\boldsymbol{x}$. However, unlike diffusion models, BFNs and BSI operate on distributions rather than single samples. While BSI has considered the Gaussian case, it is not limited to it, and we will consider categorical distributions in Sec. 3, as done by BFNs.

3 TreeGen: A Generative Model for Hierarchies

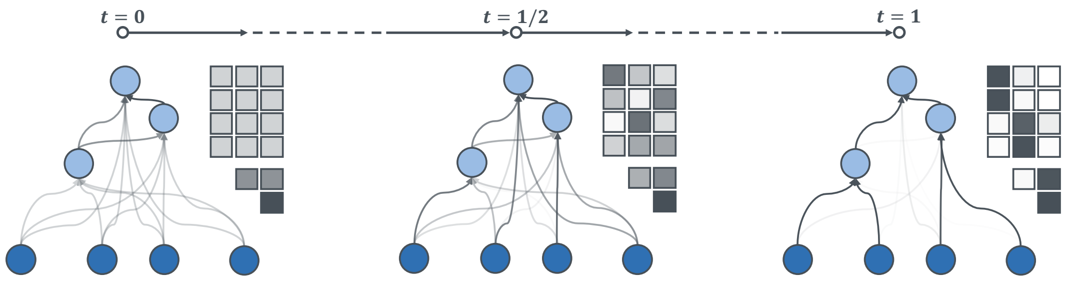

Figure 2: Overview of the TreeGen generation process. At each continuous time $t \in [0, 1]$, the model maintains a probabilistic hierarchy $\mathcal{T}_t$, applies a Bayesian-inspired update via a neural network and noisy sample, and progressively reduces entropy until converging to a discrete hierarchy $\hat{\mathcal{T}}$ at $t = 1$.

In this section, we present our main contribution: TreeGen, a Bayesian generative model designed for hierarchies. TreeGen starts from a probabilistic hierarchy $\mathcal{T}$, which is iteratively updated via Bayesian updates of observed noisy hierarchies until the entropy of the hierarchy is sufficiently low and converges toward a discrete hierarchy. To obtain noisy observations, we design a neural network trained to predict ground-truth discrete hierarchies. As such a hierarchy simply consists of a collection of categorical variables (see Sec. 2.1), we first describe the framework for arbitrary categorical distributions. While we derive update equations within the BSI framework [31], the resulting Bayesian updates match those of BFNs [19] but follow from a simpler derivation. Compared with standard BFNs, TreeGen instantiates a categorical BSI that uses the BFN update with explicit precision control while introducing a different loss, omits auxiliary distributions, and extends the parametrization to trees. We discuss these differences and provide detailed derivations in App. A.

Objective and prior. Our goal is to infer an unknown sample $x \in \{1, \ldots, K\}$. We encode our current belief about that sample via a categorical prior, i.e.,

$$p(x = k) = \pi_k, \qquad \boldsymbol{\pi} = (\pi_1, \ldots, \pi_K) \in \Delta_{K-1}, \tag{7}$$

where Δ_{K-1} is the K-simplex, i.e., $\pi_k \geq 0$ and $\sum_k \pi_k = 1$.

Noisy observation. Assume we have access to a noisy measurement vector $\mathbf{y} = (y_1, \ldots, y_K)$ sampled from a multinomial distribution with $m = \sum_k y_k$ trials and class probabilities $\boldsymbol{\theta}$, which we model as a mixture between the ground-truth Dirac distribution $\mathbf{e}_x$ and uniform noise:

$$\boldsymbol{\theta} = \omega\,\mathbf{e}_x + (1-\omega)\,\tfrac{1}{K}\mathbf{1}, \qquad 0 \leq \omega \leq 1. \tag{8}$$

$\mathbf{e}_x$ is the one-hot encoding of x and ω defines a signal–noise trade-off: $\omega = 1$ yields perfectly informative counts, while $\omega = 0$ gives pure uniform noise.

The conditional likelihood for $x = k$ is

$$p(\mathbf{y} \mid x = k, \omega) = \frac{m!}{\prod_j y_j!} \left(\tfrac{1-\omega}{K}\right)^{m-y_k} \left(\tfrac{1-\omega}{K} + \omega\right)^{y_k}. \tag{9}$$

Bayes update. After observing $\mathbf{y}$, we can update our belief on x, i.e., parameters $\boldsymbol{\pi}$ via Bayes' rule:

$$p(x = k \mid \mathbf{y}, \omega) = \frac{p(\mathbf{y} \mid x = k, \omega)\, \pi_k}{\sum_j p(\mathbf{y} \mid x = j, \omega)\, \pi_j}. \tag{10}$$

By canceling the common multinomial coefficients, we obtain a softmax-type expression:

$$p(x = k \mid \mathbf{y}, \omega) = \frac{\pi'^{\,y_k}\, \pi_k}{\sum_j \pi'^{\,y_j}\, \pi_j}, \qquad \pi' := 1 + \frac{\omega K}{1 - \omega}\ . \tag{11}$$

We can express this equivalently in vectorized form:

$$\boldsymbol{\pi}_{\text{post}} = \operatorname{softmax}\big(\log \boldsymbol{\pi} + \mathbf{y} \log \pi'\big). \tag{12}$$

This form shows that the observation contributes an additive vector $\mathbf{y} \log \pi'$ to our belief before the softmax normalization. This form also allows simple aggregation of sequential updates.

Sequential updates. With multiple independent observations $\{\mathbf{y}^{(i)}\}_{i=1}^{N}$ and constant ω, the posterior update simplifies to:

$$\boldsymbol{\pi}^{(N)} = \operatorname{softmax}\Big(\log \boldsymbol{\pi}^{(0)} + \log \pi' \sum_{i=1}^{N} \mathbf{y}^{(i)}\Big). \tag{13}$$

Thus, the class probabilities are aggregated by addition in log-space.

Gaussian interpretation. For a large observation count m, the Central Limit Theorem implies that the rescaled sum of counts is approximately Gaussian. This allows us to rewrite the Bayesian update using a Gaussian-distributed variable and in continuous time:

$$\boxed{\boldsymbol{\pi}_t = \operatorname{softmax}\big(\log \boldsymbol{\pi}_{t-1} + \mathbf{z}_t\big), \qquad \mathbf{z}_t \sim \mathcal{N}\big((\alpha_t - \alpha_{t-1})K\mathbf{e}_x, (\alpha_t - \alpha_{t-1})K\mathbf{I}\big).} \tag{14}$$

Due to the additive aggregation in log-space (see Eq. (13)), we can summarize multiple Bayesian updates into a single one, i.e., the step from $\boldsymbol{\pi}_0$ to $\boldsymbol{\pi}_t$:

$$\boxed{\boldsymbol{\pi}_t = \operatorname{softmax}\big(\mathbf{z}_t\big), \qquad \mathbf{z}_t \sim \mathcal{N}(\alpha_t K \mathbf{e}_x, \alpha_t K \mathbf{I}),} \tag{15}$$

where α_t represents the accumulated signal. Note that we omitted $\log \boldsymbol{\pi}_0$ as it is constant and the softmax operation is shift invariant. Consequently, the log-evidence in the softmax follows a Gaussian and is parametrized with α_t. The recovered updates equal those of Graves et al. [19].

Distribution of $\boldsymbol{\pi}_t$. Following the categorical BFN formulation, we represent the belief vector at time t as the softmax of latent Gaussian logits, $\boldsymbol{\pi}_t = \operatorname{softmax}(\mathbf{z}_t)$ conditioned on the ground-truth class x. This results in the distribution:

$$p(\boldsymbol{\pi}_t \mid \boldsymbol{\pi}_{t-1}, \mathbf{x}) = \int \delta\big(\boldsymbol{\pi}_t - \operatorname{softmax}(\mathbf{z}_t)\big)\, p(\mathbf{z}_t \mid \mathbf{x}, \alpha_t, \alpha_{t-1})\, \mathrm{d}\mathbf{z}_t, \tag{16}$$

Furthermore, we can model the marginal of $\boldsymbol{\pi}_t$ directly without intermediate steps:

$$p(\boldsymbol{\pi}_t \mid \mathbf{x}) = \int \delta\big(\boldsymbol{\pi}_t - \operatorname{softmax}(\mathbf{z}_t)\big)\, p(\mathbf{z}_t \mid \mathbf{x}, \alpha_t)\, \mathrm{d}\mathbf{z}_t. \tag{17}$$

Both distributions are trivial to sample by drawing $\mathbf{z}_t$ from the corresponding Gaussian and applying the softmax. During generation, the true class x is unknown, so we replace it with a proxy $\hat{x} = \boldsymbol{f}_{\boldsymbol{\theta}}(\boldsymbol{\pi}_t, t)$ predicted by our neural network and approximate the one-step transition by $p_\theta(\boldsymbol{\pi}_t \mid \boldsymbol{\pi}_{t-1}) = p(\boldsymbol{\pi}_t \mid \boldsymbol{f}_{\boldsymbol{\theta}}(\boldsymbol{\pi}_t, t))$, which recovers the distribution of $\boldsymbol{\pi}_t$ when $f_{\boldsymbol{\theta}}(\boldsymbol{\pi}_t, t)$ successfully predicts x. Unlike the BFN update, this allows us to control the precision directly.

Training of the neural network $f_\theta(\pi_t, t)$. Our goal is to train the network to recover the original sample x from a categorical distribution π_t. Therefore, at each training step we draw a ground-truth sample x from the dataset $\mathcal{D}$ and a timestep $t \sim \mathcal{U}(0,1)$, then sample the corresponding distribution π_t according to Eq.(15). The network receives π_t and t as inputs, and outputs a categorical distribution, aiming to concentrate all probability mass on the true class x. We optimize the parameters θ by minimizing the expected cross-entropy loss:

$$\mathcal{L}(\theta) = \mathbb{E}_{x\sim\mathcal{D}, t\sim\mathcal{U}(0,1), \pi_t \sim p_t(\pi_t|\mathbf{x})} \Big[\mathrm{CELoss}\big(f_\theta(\pi_t, t),\, x\big)\Big], \tag{18}$$

where CELoss denotes the cross-entropy loss between the predicted categories and the ground-truth label. The nested expectation is approximated with Monte-Carlo samples of x, t, and π_t in each minibatch, and gradients are propagated through the network to update θ.

Entropy scheduler. During generation, we want the entropy of π_t to decrease smoothly from its maximum (uniform) value to zero (one-hot). If we draw

$$\mathbf{z}_t \sim \mathcal{N}\big(\alpha_t K \mathbf{e}_x, \alpha_t K \mathbf{I}\big),$$
$$\pi_t = \mathrm{softmax}(\mathbf{z}_t),$$

then the entropy of π_t is a monotone function of α_t. While BFNs [19] chose $\alpha_t = Ct^2$, the constant C requires retuning when the number of classes K changes. We instead propose

$$\alpha_t = -\frac{C + a\log_2 K}{K}\ln(1-t), \tag{19}$$

for $t \in [0,1]$, which yields an *approximately linear* decay of expected normalized entropy (see Fig. 3) while ensuring π_0 is uniform and $\pi_1 = \mathbf{e}_x$. Because our experiments span hierarchies with varying numbers of classes (see Sec. 2.1), this scheduler enables us to use the *same* hyperparameters across all sizes of hierarchies.

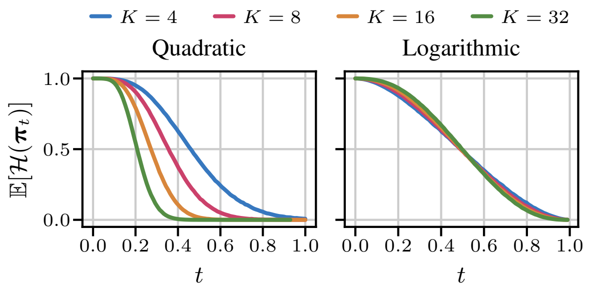

Figure 3: Comparison of entropy schedulers. The plots show the expected normalized entropy of the categorical belief π_t over time t, for varying class counts K. **Left:** the quadratic schedule used in standard BFNs. **Right:** our proposed log-based schedule, which yields an approximately linear decay across different K.

Adaptation to hierarchies. Extending the categorical generation from a single random variable to an entire hierarchy means treating every row of $(\boldsymbol{A}, \boldsymbol{B})$ as its own categorical distribution, while updating all rows *jointly* so that the resulting sample is a valid hierarchy. Concretely, we model the n rows of $\boldsymbol{A}$ and the n' rows of the upper-triangular matrix $\boldsymbol{B}$ as categorical distributions, where each class represents a parent choice for a node. Note that K, i.e., the number of possible parents, varies with hierarchy size and across rows of $\boldsymbol{B}$ due to the upper-triangular structure. This parametrization induces a distribution over rooted trees (hierarchies) and substantially reduces the search space compared to arbitrary graph generation. Accordingly, f_θ takes the current probabilistic hierarchy $\mathcal{T}_t = (\boldsymbol{A}_t, \boldsymbol{B}_t)$ and outputs a discrete proposal $\hat{\mathcal{T}}$. This prediction is then used to update the current belief, i.e., the probabilistic hierarchy, using Eq. (15). We show algorithms for sampling and training in Algs. 1 and 2, respectively.

Algorithm 1 Sampling with TreeGen

```
input: Neural network $f_\theta$, entropy schedule $\alpha_t$ for $t \in [0,1]$, sampling steps $N$
output: Discrete hierarchy $\mathcal{T}_1$
1: $\mathcal{T}_0 = 1/K$
2: for $t$ in $\{1/N, \dots, 1\}$ do
3:     $\hat{\mathcal{T}} \leftarrow f_\theta(\mathcal{T}_{t-1/N}, t - 1/N)$        ▷ Evaluate $f_\theta$
4:     $\mathbf{z}_t \sim \mathcal{N}\big(\alpha_t K \hat{\mathcal{T}}, \alpha_t K \mathbf{I}\big)$        ▷ Eq. (15)
5:     $\mathcal{T}_t \leftarrow \mathrm{softmax}(\mathbf{z}_t)$        ▷ Eq. (15)
6: end for
7: return $\mathcal{T}_1$
```

Algorithm 2 Training TreeGen

```
input: Dataset $\mathcal{D}$, neural network $f_\theta$, entropy schedule $\alpha_t$ for $t \in [0,1]$, training steps $N$
1: for $n = 1$ to $N$ do
2:     $\mathcal{T} \sim \mathcal{D}, t \sim \mathcal{U}(0,1)$
3:     $\mathbf{z}_t \sim \mathcal{N}\big(\alpha_t K \mathcal{T},\ \alpha_t K \mathbf{I}\big)$        ▷ Eq. (15)
4:     $\mathcal{T}_t \leftarrow \mathrm{softmax}(\mathbf{z}_t)$        ▷ Eq. (15)
5:     $\hat{\mathcal{T}} \leftarrow f_\theta(\mathcal{T}_t,\ t)$        ▷ Evaluate $f_\theta$
6:     $\mathcal{L} \leftarrow \mathrm{CE}\big(\hat{\mathcal{T}}, \mathcal{T}\big)$        ▷ Compute loss
7:     $\theta \leftarrow \theta - \eta\, \nabla_\theta \mathcal{L}$        ▷ Gradient step
8: end for
```

4 Experiments

In this section, we present our empirical results on the jet-clustering task. Our primary goal is to demonstrate the effectiveness of TreeGen in generating valid hierarchies adhering to the true data distribution. We compare TreeGen against various baselines and test how well the generated hierarchies approximate the ground-truth posterior distributions.

We evaluate TreeGen on hierarchies derived from the GINKGO dataset, focusing on QCD and W jets. More specifically, our experiments focus on the conditional generation $p(\mathcal{T} \mid \boldsymbol{X})$, where $\boldsymbol{X}$ are leaf features. Finally, we conduct ablation studies to analyze the impact of key design choices in our method in App. C.

4.1 Experimental Setup

Datasets. Our evaluation uses five datasets obtained with the GINKGO jet shower generator [12]: **QCD jets:** QCD-S, QCD-M, QCD-L, and **W-Boson jets:** W-S, W-M. All five share the same root four-momentum p^{μ}_{root} and decay rate λ, but vary in the shower cut-off Δ_{cut}, controlling the final jet size. The datasets have $\Delta_{\text{cut}} \in \{4.0^2,\ 1.1^2,\ 0.6^2\}$ and contain hierarchies with at most 19 (small), 59 (medium), and 99 (large) nodes. Each dataset consists of 100,000 hierarchies. Split into 98,000 hierarchies for training and 1,000 for validation and testing. In our setup, the leaves of the hierarchies correspond to the observed particles with features $\mathbf{X}$, while internal nodes are latent and to be inferred via the sampled hierarchy $\mathcal{T}$. Fig. 8 shows the leaf-count distribution for the three QCD datasets. We provide more details about the datasets and task in App. B.2.

Baselines. We benchmark the generative capabilities of TreeGen against various baselines. We include CatFlow [16] and (standard) Bayesian Flow Networks (BFNs) [19] representing state-of-the-art generative models for categorical data. Furthermore, we compare to greedy clustering approaches and the ground-truth posterior obtained via cluster trellis [33]. Finally, we compare to the CA [15, 46], k_T [17], and anti-k_T [7] algorithms in App. C, representing traditional jet clustering algorithms. All generative baselines share the tree assumption (see Sec. 2.1), while the agglomerative algorithms are tailored to jet clustering and restricted to binary hierarchies. We describe the baselines in more detail in App. B.5.

Evaluation metrics. To assess the performance of the generative model, we employ two metrics. First, we compute the — valid hierarchies — fraction of generated hierarchies that satisfy dataset-specific constraints, i.e., required physical properties. Second, we assess how well the sampled hierarchies match the data distribution by comparing their log-likelihoods to those of the ground-truth hierarchies. Specifically, we compute the ratio of log-likelihoods of each generated hierarchy to its corresponding ground-truth counterpart and report the average ratio over the test set. A ratio close to one indicates that the model closely approximates the true data distribution. We discuss further details about both metrics in App. B.6.

Practical considerations. TreeGen requires an architecture that predicts a hierarchy given a probabilistic hierarchy as input. This structure makes it suitable for a Graph Transformer [38]. We fix $n' = n - 1$, i.e., one parent for every non-root node, as we operate on binary hierarchies. We depict the high-level architecture in Fig. 4 and provide more details in App. B.3 and discuss node and edge features in App. B.4. We train all models using Adam [28] with a learning rate of 0.0001 and gradient clipping set to 0.5 for 50 epochs. For generation, all models use 1000 steps, except for the ablation in Fig. 7, where all use 100. We provide an overview of all hyperparameters in App. B.1. Finally, we report the mean and standard deviation of four random seeds for all experiments to ensure reproducibility.

4.2 Results

Hierarchy generation. We report the fraction of valid trees and log-likelihoods in Tab. 1. TreeGen generates *nearly perfect* trees in every case, achieving ≥ 0.93 validity and likelihood ratios close to one, consistently outperforming baselines across all datasets. By contrast, CatFlow and BFN deteriorate rapidly as jet size grows: on the medium QCD set, their valid-tree fractions drop to 0.24 and 0.65, respectively. We attribute CatFlow's inferior performance to its flow leaving the

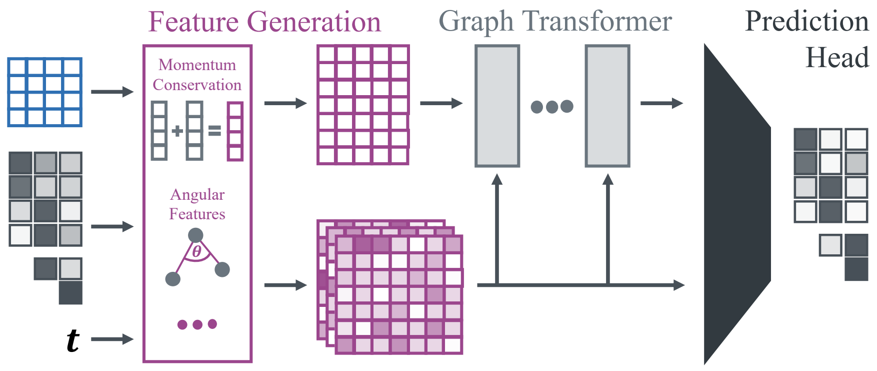

Figure 4: TreeGen model architecture. Node and edge features (structural and physics-inspired) are derived from the current probabilistic hierarchy, then processed by a Graph Transformer to predict the parameters of the final hierarchy $\mathcal{T}_1$.

probability simplex: intermediate states can violate the categorical constraints that define a valid jet hierarchy. The Bayesian-based approaches BFN and TreeGen remain on the simplex throughout generation by design. These results show that TreeGen's successfully scales to larger, more complex jets, consistently maintaining both the highest validity and the best log-likelihood fractions.

Table 1: Evaluation metrics for different models across datasets. Best scores in **bold**.

Dataset	CatFlow		BFN		TreeGen	
	Valid Frac. (↑)	LLH Frac.	Valid Frac. (↑)	LLH Frac.	Valid Frac. (↑)	LLH Frac.
QCD-S	$0.752_{\pm 0.014}$	$0.972_{\pm 0.002}$	$0.941_{\pm 0.003}$	$0.982_{\pm 0.000}$	$\mathbf{0.997}_{\pm 0.001}$	$\mathbf{1.003}_{\pm 0.002}$
QCD-M	$0.236_{\pm 0.016}$	$0.882_{\pm 0.003}$	$0.645_{\pm 0.040}$	$0.936_{\pm 0.002}$	$\mathbf{0.977}_{\pm 0.010}$	$\mathbf{0.994}_{\pm 0.002}$
QCD-L	-	-	$0.416_{\pm 0.036}$	$0.898_{\pm 0.002}$	$\mathbf{0.943}_{\pm 0.016}$	$\mathbf{0.975}_{\pm 0.001}$
W-S	$0.604_{\pm 0.014}$	$0.937_{\pm 0.007}$	$0.851_{\pm 0.014}$	$0.965_{\pm 0.001}$	$\mathbf{0.994}_{\pm 0.002}$	$\mathbf{1.006}_{\pm 0.001}$
W-M	-	-	$0.341_{\pm 0.054}$	$0.886_{\pm 0.002}$	$\mathbf{0.930}_{\pm 0.024}$	$\mathbf{0.980}_{\pm 0.004}$

Furthermore, Fig. 5 visualizes the *per-tree* log-likelihoods: each dot compares the log-likelihood of the ground-truth hierarchy (x-axis) with the log-likelihood of the hierarchy generated by our model (y-axis). TreeGen's points cluster along the diagonal, indicating alignment with the true distributions. This confirms that TreeGen not only produces more valid hierarchies but faithfully reproduces the likelihoods of the ground-truth.

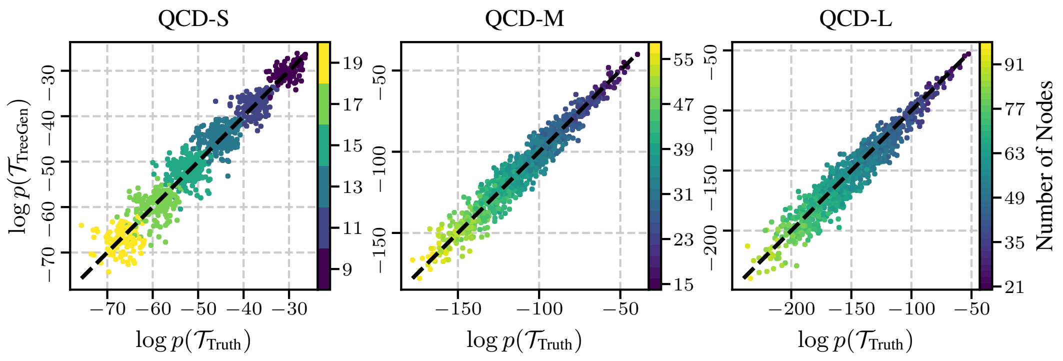

Figure 5: Scatter plot of log-likelihoods. Each point corresponds to a test hierarchy: the x-axis shows the log-likelihood of true hierarchy, and the y-axis shows the log-likelihood hierarchy generated by TreeGen, demonstrating close alignment across varying hierarchy sizes.

Posterior distribution. While our reported quantitative metrics demonstrate that TreeGen produces reasonable hierarchies, they do not directly assess how well it approximates the true posterior $p(\mathcal{T} \mid \boldsymbol{X})$. To complement our evaluation, we employ the cluster trellis data structure [33] to draw exact samples from the posterior. This enables us to compare these samples with those generated by TreeGen. Since the computational complexity of cluster trellis scales exponentially as $\mathcal{O}(3^N)$, this evaluation is only feasible for the QCD-S dataset, which contains hierarchies of up to 20 nodes. For each of the 1000 test hierarchies, we draw one sample from the true posterior via cluster trellis and one from TreeGen.

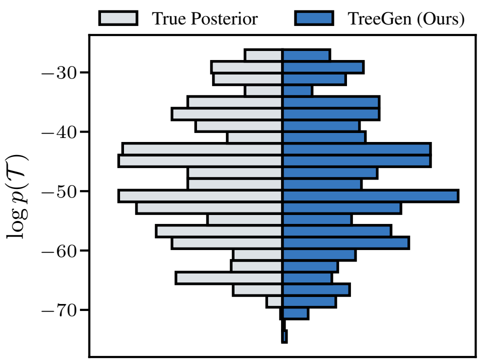

Figure 6: Histogram of posterior log-likelihoods. Distributions of $\log p(\mathcal{T} \mid X)$ for true hierarchies versus TreeGen-sampled hierarchies, demonstrating that TreeGen successfully approximates the full posterior.

We visualize and compare the empirical distributions over the log-likelihoods using histograms in Fig. 6. The empirical distribution produced by our generative model successfully captures the key characteristics of the true posterior distribution. This further validates TreeGen's ability to accurately learn and represent hierarchical structures.

Likelihood Maximization. While sampling from TreeGen provides diverse plausible reconstructions, many applications require a single high-likelihood hierarchy. Our model's non-deterministic nature allows us to resample hierarchies multiple times. To this end, we perform approximate MAP inference via rejection sampling. More specifically, for each jet event X, we draw N independent hierarchies $\{\hat{\mathcal{T}}_i\}_{i=1}^{N} \sim p_\theta(\hat{\mathcal{T}} \mid \mathbf{X})$, compute their log-likelihoods $\log p(\hat{\mathcal{T}}_i)$, and select the sample with the highest value. We benchmark this against a deterministic greedy agglomerative linkage algorithm that merges clusters by maximizing local likelihood gains. In Fig. 7, we show how the log-likelihood grows with the number of samples N compared to the generative baselines and the greedy algorithm.

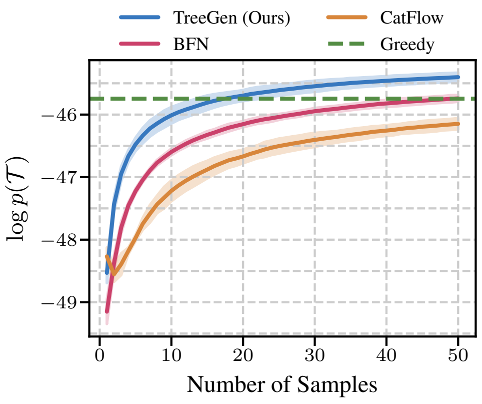

Figure 7: Likelihood maximization. Maximum log-likelihood obtained by drawing N candidate hierarchies from TreeGen and the log-likelihood of the deterministic greedy reconstruction. TreeGen outperforms the baseline within a few samples.

We observe that the log-likelihood obtained by TreeGen exceeds that of the greedy agglomerative baseline after only 16 samples and consistently outperforms CatFlow and BFN, demonstrating that our samples not only concentrate around higher-probability hierarchies but also capture diversity beyond a single greedy pass. Note that both this rejection-sampling MAP procedure and the greedy likelihood clustering assume access to the exact likelihood, which is often unknown or intractable for realistic collision data. Nevertheless, this experiment highlights the practical benefit of our model's ability to sample multiple hierarchies, enabling improved reconstruction quality whenever quantitative evaluations are available.

Scheduler comparison. We compare our scheduler, proposed in Sec. 3, with the BFN scheduler [19] across different C. Following Graves et al. [19], we include $C = 0.75$ and $C = 3.0$. Additionally, we test $C = 6.0$ and $C = 9.0$. The results on QCD-S are shown in Tab. 2.

Table 2: Scheduler ablation on validity and LLH fraction.

Scheduler	Valid Frac. (↑)	LLH Frac.
Ours	0.997 ± 0.001	1.003 ± 0.002
C = 0.75	0.410 ± 0.019	0.990 ± 0.002
C = 3.0	0.989 ± 0.001	1.002 ± 0.002
C = 6.0	0.994 ± 0.001	1.003 ± 0.002
C = 9.0	0.992 ± 0.004	1.002 ± 0.001

As we observe, the scheduler of Graves et al. [19] is highly sensitive to C. While $C = 0.75$ highly degrades validity, larger values result in matching performance to ours.

5 Related Work

5.1 Hierarchical Clustering

Agglomerative algorithms iteratively merge clusters based on the shortest distance, building a hierarchy from individual points until converged to a single cluster. Different choices to define the inter-cluster distance give rise to various linkage algorithms [21]. Divisive algorithms proceed in reverse and build hierarchies by splitting a single cluster, containing all points, into smaller and smaller clusters, e.g., by repeatedly applying the k-means algorithm [43] or spectral clustering [14].

Recently proposed cost functions, such as the Dasgupta cost [14] and the Tree Sampling Divergence (TSD) [10], have enabled global optimization across the entire hierarchy. While these cost functions remain infeasible to optimize directly, various continuous relaxations have been proposed to allow for gradient-based optimization [11, 34, 9, 48, 30]. These methods then optimize relaxed objectives.

Similar to hierarchical clustering algorithms, TreeGen aims to infer hierarchies and shares the same parametrization for probabilistic hierarchies as Zügner et al. [48] and Kollovieh et al. [30]. However, we focus on a supervised setting and learn a distribution of hierarchies, whereas the former focuses on inferring hierarchies based on heuristics or objective functions.

5.2 Jet Clustering

Jet clustering is a well-studied task in high-energy physics. Initially, cone algorithms [5], which select the most energetic particles and group all particles within a cone around them, were employed for this task. However, these algorithms were sensitive to low-energy particles [29]. This limitation led to the development of sequential recombination clustering algorithms, which are instances of agglomerative hierarchical clustering. Different algorithms in this class, such as the Cambridge/Aachen algorithm [15, 46], the k_T algorithm [17], and the anti-k_T algorithm [7], differ in how they combine angular proximity and energy of particles into a distance measure.

Recently, the development of the GINKGO simulator [12] introduced a new class of algorithms that use this simulator to assess the likelihood of splits in the hierarchy, aiming to find the hierarchy with the maximum likelihood [6, 20, 33, 13]. Among those, cluster trellis [33] is most similar to our method as it enables sampling from the exact posterior distribution for small hierarchies. However, our model learns directly from simulator-generated data without requiring likelihood evaluations at inference time, which allows it to be applied with any black-box simulator. Finally, Yang et al. [47] propose a variational-inference method for jet clustering on the GINKGO dataset.

5.3 Generative Models

Our work builds on recent advances in generative modeling, particularly diffusion and flow-matching frameworks. Diffusion models add random noise to data and then learn to reverse this diffusion process to generate samples starting from noise [39, 23, 40, 41]. Flow matching generalizes this idea by directly learning an ODE that transforms data to noise via regression of vector fields [32]. Furthermore, Graves et al. [19] introduced BFNs, another related generative framework that maintains and updates a probability distribution during generation in a Bayesian manner rather than acting directly on the sample. Atkinson et al. [1] proposed an ODE-based BFN sampling algorithm that replaces aggregated previous predictions with the most recent prediction, also providing explicit precision control, similar to ours.

Generative models for discrete data are particularly relevant to our approach since hierarchies are discrete structures. One class of such models maintains discreteness throughout the generative process. Various approaches have adapted diffusion models to discrete data [24, 2, 8]. Recent flow matching approaches confine the generative process in continuous space. For example, Dirichlet Flow Matching [42] constrains the process on the probability simplex, while CatFlow [16] removes this constraint, allowing values outside the simplex. Our approach belongs to the former category, as we build upon the BFN framework, transitioning between categorical distributions.

Prior work, such as the junction tree autoencoder [25], modeled trees in an autoregressive fashion for molecule generation. Other approaches used diffusion and flow matching for general graph generation [35, 26, 45, 16]. Unlike these, however, our framework explicitly parametrizes valid hierarchies (rather than distributions over all graphs), substantially reducing the search space.

6 Conclusion

In this work, we introduced TreeGen, a novel generative model learning hierarchies from distributions building upon the BFN [19] and BSI [31] framework. By proposing an entropy scheduler, we are able to model categorical variables smoothly across a varying number of classes. The intermediate states of the generation process are probabilistic hierarchies, which we used to derive meaningful features, improving generative performance.

We assessed TreeGen on a high-energy jet simulator benchmark and found that close to 100% of the generated hierarchies adhere to their corresponding physical properties. Moreover, by comparing the likelihoods of conditionally generated hierarchies to those of the ground truth, we demonstrated that our model is able to successfully approximate the posterior distribution.

Limitations and future work. A core component of our generative model is a graph transformer whose computational complexity increases quadratically with the number of nodes. This issue arises from the densely connected probabilistic hierarchies during generation.

To this end, we have evaluated TreeGen on GINKGO [12] as it provides analytical likelihood computations. Immediate extensions include evaluating TreeGen on different simulators [3, 4] and experimental, i.e., real-world jet datasets, where measurement noise and detector effects introduce additional complexity. TreeGen naturally extends to non-binary trees by adjusting the number of internal nodes n' (for binary trees $n-1$). Potential strategies include sampling n' (as in molecule generation) [45]; predicting n' using a classifier similar to Kerrigan et al. [27]; or setting a larger n' and pruning unused internal nodes, as done in hierarchical clustering [48]. Finally, one could explore alternative hierarchy parameterizations enforcing strict binary-tree constraints or improving both computational efficiency and likelihoods.

Contributions

MK developed the project idea, derived the theory, implemented the core method, and wrote the manuscript. NF implemented most of the experimental pipeline (data loading, features, backbone, baselines, training, and evaluation) and assisted with the manuscript. FG supervised the neural network architecture design. BS contributed to conceiving the initial idea. SG contributed to the method design and provided overall scientific guidance. All authors discussed results, both theoretical and empirical, and revised the manuscript.

Acknowledgments

We thank Johanna Sommer for valuable feedback on the idea and Marten Lienen for help with the background section.

References

[1] Timothy Atkinson, Thomas D Barrett, Scott Cameron, Bora Guloglu, Matthew Greenig, Charlie B Tan, Louis Robinson, Alex Graves, Liviu Copoiu, and Alexandre Laterre. Protein sequence modelling with bayesian flow networks. *Nature Communications*, 16(1):3197, 2025.

[2] Jacob Austin, Daniel D Johnson, Jonathan Ho, Daniel Tarlow, and Rianne Van Den Berg. Structured denoising diffusion models in discrete state-spaces. *Advances in neural information processing systems*, 34:17981–17993, 2021.

[3] Johannes Bellm, Stefan Gieseke, David Grellscheid, Simon Plätzer, Michael Rauch, Christian Reuschle, Peter Richardson, Peter Schichtel, Michael H Seymour, Andrzej Siódmok, et al. Herwig 7.0/herwig++ 3.0 release note. *The European Physical Journal C*, 76:1–8, 2016.

[4] Christian Bierlich, Smita Chakraborty, Nishita Desai, Leif Gellersen, Ilkka Helenius, Philip Ilten, Leif Lönnblad, Stephen Mrenna, Stefan Prestel, Christian Tobias Preuss, et al. A comprehensive guide to the physics and usage of pythia 8.3. *SciPost Physics Codebases*, page 008, 2022.

[5] Gerald C Blazey, Jay R Dittmann, Stephen D Ellis, V Daniel Elvira, K Frame, S Grinstein, Robert Hirosky, R Piegaia, H Schellman, R Snihur, et al. Run ii jet physics: proceedings of the run ii qcd and weak boson physics workshop. *arXiv preprint hep-ex/0005012*, 2000.

[6] Johann Brehmer, Sebastian Macaluso, Duccio Pappadopulo, and Kyle Cranmer. Hierarchical clustering in particle physics through reinforcement learning. *arXiv preprint arXiv:2011.08191*, 2020.

[7] Matteo Cacciari, Gavin P Salam, and Gregory Soyez. The anti-kt jet clustering algorithm. *Journal of High Energy Physics*, 2008(04):063, 2008.

[8] Andrew Campbell, Joe Benton, Valentin De Bortoli, Thomas Rainforth, George Deligiannidis, and Arnaud Doucet. A continuous time framework for discrete denoising models. *Advances in Neural Information Processing Systems*, 35:28266–28279, 2022.

[9] Ines Chami, Albert Gu, Vaggos Chatziafratis, and Christopher Ré. From trees to continuous embeddings and back: Hyperbolic hierarchical clustering. *Advances in Neural Information Processing Systems*, 33:15065–15076, 2020.

[10] Bertrand Charpentier and Thomas Bonald. Tree sampling divergence: an information-theoretic metric for hierarchical graph clustering. In *IJCAI-19*, 2019.

[11] Giovanni Chierchia and Benjamin Perret. Ultrametric fitting by gradient descent. *Advances in neural information processing systems*, 32, 2019.

[12] Kyle Cranmer, Sebastian Macaluso, and Duccio Pappadopulo. Toy generative model for jets. URL https://github.com/SebastianMacaluso/ginkgo/blob/master/notes/toyshower_v4.pdf.

[13] Kyle Cranmer, Matthew Drnevich, Sebastian Macaluso, and Duccio Pappadopulo. Reframing jet physics with new computational methods. In *EPJ Web of Conferences*, volume 251, page 03059. EDP Sciences, 2021.

[14] Sanjoy Dasgupta. A cost function for similarity-based hierarchical clustering. In *Proceedings of the forty-eighth annual ACM symposium on Theory of Computing*, pages 118–127, 2016.

[15] Yu L Dokshitzer, GD Leder, S Moretti, and BR Webber. Better jet clustering algorithms. *Journal of High Energy Physics*, 1997(08):001, 1997.

[16] Floor Eijkelboom, Grigory Bartosh, Christian Andersson Naesseth, Max Welling, and Jan-Willem van de Meent. Variational flow matching for graph generation. *Advances in Neural Information Processing Systems*, 37:11735–11764, 2024.

[17] Stephen D Ellis and Davison E Soper. Successive combination jet algorithm for hadron collisions. *Physical Review D*, 48(7):3160, 1993.

[18] J. Felsenstein. *Inferring phylogenies*. Sinauer Associates, 2003.

[19] Alex Graves, Rupesh Kumar Srivastava, Timothy Atkinson, and Faustino Gomez. Bayesian flow networks. *arXiv preprint arXiv:2308.07037*, 2023.

[20] Craig S Greenberg, Sebastian Macaluso, Nicholas Monath, Avinava Dubey, Patrick Flaherty, Manzil Zaheer, Amr Ahmed, Kyle Cranmer, and Andrew McCallum. Exact and approximate hierarchical clustering using a. In *Uncertainty in Artificial Intelligence*, pages 2061–2071. PMLR, 2021.

[21] Trevor Hastie, Robert Tibshirani, Jerome H Friedman, and Jerome H Friedman. *The elements of statistical learning: data mining, inference, and prediction*, volume 2. Springer, 2009.

[22] Geoffrey Hinton. How to represent part-whole hierarchies in a neural network. *Neural Computation*, 35(3):413–452, 2023.

[23] Jonathan Ho, Ajay Jain, and Pieter Abbeel. Denoising diffusion probabilistic models. *Advances in neural information processing systems*, 33:6840–6851, 2020.

[24] Emiel Hoogeboom, Didrik Nielsen, Priyank Jaini, Patrick Forré, and Max Welling. Argmax flows and multinomial diffusion: Learning categorical distributions. *Advances in neural information processing systems*, 34:12454–12465, 2021.

[25] Wengong Jin, Regina Barzilay, and Tommi Jaakkola. Junction tree variational autoencoder for molecular graph generation. In *International conference on machine learning*, pages 2323–2332. PMLR, 2018.

[26] Jaehyeong Jo, Seul Lee, and Sung Ju Hwang. Score-based generative modeling of graphs via the system of stochastic differential equations. In *International conference on machine learning*, pages 10362–10383. PMLR, 2022.

[27] Gavin Kerrigan, Kai Nelson, and Padhraic Smyth. Eventflow: Forecasting temporal point processes with flow matching. *arXiv preprint arXiv:2410.07430*, 2024.

[28] Diederik P Kingma and Jimmy Ba. Adam: A method for stochastic optimization. *arXiv preprint arXiv:1412.6980*, 2014.

[29] Roman Kogler, Benjamin Nachman, Alexander Schmidt, Lily Asquith, Emma Winkels, Mario Campanelli, Chris Delitzsch, Philip Harris, Andreas Hinzmann, Deepak Kar, et al. Jet substructure at the large hadron collider. *Reviews of Modern Physics*, 91(4):045003, 2019.

[30] Marcel Kollovieh, Bertrand Charpentier, Daniel Zügner, and Stephan Günnemann. Expected probabilistic hierarchies. *Advances in Neural Information Processing Systems*, 37:13818–13850, 2024.

[31] Marten Lienen, Marcel Kollovieh, and Stephan Günnemann. Generative modeling with bayesian sample inference. *arXiv preprint arXiv:2502.07580*, 2025.

[32] Yaron Lipman, Ricky TQ Chen, Heli Ben-Hamu, Maximilian Nickel, and Matt Le. Flow matching for generative modeling. *arXiv preprint arXiv:2210.02747*, 2022.

[33] Sebastian Macaluso, Craig Greenberg, Nicholas Monath, Ji Ah Lee, Patrick Flaherty, Kyle Cranmer, Andrew McGregor, and Andrew McCallum. Cluster trellis: Data structures & algorithms for exact inference in hierarchical clustering. In *International Conference on Artificial Intelligence and Statistics*, pages 2467–2475. PMLR, 2021.

[34] Nicholas Monath, Manzil Zaheer, Daniel Silva, Andrew McCallum, and Amr Ahmed. Gradient-based hierarchical clustering using continuous representations of trees in hyperbolic space. In *Proceedings of the 25th ACM SIGKDD International Conference on Knowledge Discovery & Data Mining*, pages 714–722, 2019.

[35] Chenhao Niu, Yang Song, Jiaming Song, Shengjia Zhao, Aditya Grover, and Stefano Ermon. Permutation invariant graph generation via score-based generative modeling. In *International conference on artificial intelligence and statistics*, pages 4474–4484. PMLR, 2020.

[36] Fabian Pedregosa, Gaël Varoquaux, Alexandre Gramfort, Vincent Michel, Bertrand Thirion, Olivier Grisel, Mathieu Blondel, Peter Prettenhofer, Ron Weiss, Vincent Dubourg, et al. Scikit-learn: Machine learning in python. *Journal of machine learning research*, 12(Oct):2825–2830, 2011.

[37] Erzsébet Ravasz and Albert Ĺaszló Barabási. Hierarchical organization in complex networks. *Physical review. E, Statistical, nonlinear, and soft matter physics*, 67 2 Pt 2:026112, 2002.

[38] Yunsheng Shi, Zhengjie Huang, Shikun Feng, Hui Zhong, Wenjin Wang, and Yu Sun. Masked label prediction: Unified message passing model for semi-supervised classification. *arXiv preprint arXiv:2009.03509*, 2020.

[39] Jascha Sohl-Dickstein, Eric Weiss, Niru Maheswaranathan, and Surya Ganguli. Deep unsupervised learning using nonequilibrium thermodynamics. In *International conference on machine learning*, pages 2256–2265. pmlr, 2015.

[40] Yang Song and Stefano Ermon. Generative modeling by estimating gradients of the data distribution. *Advances in neural information processing systems*, 32, 2019.

[41] Yang Song, Jascha Sohl-Dickstein, Diederik P Kingma, Abhishek Kumar, Stefano Ermon, and Ben Poole. Score-based generative modeling through stochastic differential equations. *arXiv preprint arXiv:2011.13456*, 2020.

[42] Hannes Stark, Bowen Jing, Chenyu Wang, Gabriele Corso, Bonnie Berger, Regina Barzilay, and Tommi Jaakkola. Dirichlet flow matching with applications to dna sequence design. In *International Conference on Machine Learning*, pages 46495–46513. PMLR, 2024.

[43] Michael Steinbach, George Karypis, and Vipin Kumar. A comparison of document clustering techniques. 2000.

[44] Ashish Vaswani, Noam Shazeer, Niki Parmar, Jakob Uszkoreit, Llion Jones, Aidan N Gomez, Łukasz Kaiser, and Illia Polosukhin. Attention is all you need. *Advances in neural information processing systems*, 30, 2017.

[45] Clément Vignac, Igor Krawczuk, Antoine Siraudin, Bohan Wang, Volkan Cevher, and Pascal Frossard. Digress: Discrete denoising diffusion for graph generation. In *ICLR*, 2023.

[46] Markus Wobisch and Thorsten Wengler. Hadronization corrections to jet cross sections in deep-inelastic scattering. *arXiv preprint hep-ph/9907280*, 1999.

[47] Hanming Yang, Antonio Khalil Moretti, Sebastian Macaluso, Philippe Chlenski, Christian A. Naesseth, and Itsik Pe'er. Variational pseudo marginal methods for jet reconstruction in particle physics. *Transactions on Machine Learning Research*, 2024. ISSN 2835-8856.

[48] Daniel Zügner, Bertrand Charpentier, Morgane Ayle, Sascha Geringer, and Stephan Günnemann. End-to-end learning of probabilistic hierarchies on graphs. In *International Conference on Learning Representations*, 2021.

A Theory

In the following, we will provide derivations for equations Eqs. (13) to (15). Both theorems build on the theory of Bayesian Flow Networks and summarize the derivations from Graves et al. [19].

Theorem A.1. *Let $x \in \{1, \dots, K\}$ have prior $\boldsymbol{\pi}^{(0)} \in \Delta_{K-1}$. For each update $i = 1, \dots, N$ we observe $\mathbf{y}^{(i)} = (y_1^{(i)}, \dots, y_K^{(i)}) \in \mathbb{N}^K$, with total count $m = \sum_k y_k^{(i)}$, sampled from*

$$p(\mathbf{y} \mid x = k, \omega) = \frac{m!}{\prod_j y_j!} \left(\tfrac{1-\omega}{K}\right)^{m-y_k} \left(\tfrac{1-\omega}{K} + \omega\right)^{y_k}, \qquad \omega \in (0,1). \tag{20}$$

Then the posterior after N sequential Bayesian updates is

$$\boldsymbol{\pi}^{(N)} = \operatorname{softmax}\Big(\log \boldsymbol{\pi}^{(0)} + \mathbf{y} \log \pi'\Big), \tag{21}$$

where $\pi' := 1 + \frac{\omega K}{1-\omega}$ and $\mathbf{y}$ the sum of N samples, i.e., $\mathbf{y} := \sum_{i=1}^N \mathbf{y}^{(i)}$.

Proof. We prove by induction on N.

Base case ($N = 1$). By Bayes' rule for a single observation $\mathbf{y}^{(1)}$,

$$\begin{aligned}
\pi_k^{(1)} &= p(x = k \mid \mathbf{y}^{(1)}; \omega) && (22)\\
&= \frac{p(\mathbf{y}^{(1)} \mid x = k; \omega)\pi_k^{(0)}}{\sum_{k'=1}^K p(\mathbf{y}^{(1)} \mid x = k'; \omega)\pi_{k'}^{(0)}} && (23)\\
&= \frac{\frac{m!}{\prod_{j=1}^K y_j!} \left[\frac{1-\omega}{K}\right]^{m-y_k^{(1)}} \left[\frac{1-\omega}{K} + \omega\right]^{y_k^{(1)}} \pi_k^{(0)}}{\sum_{k'=1}^K \frac{m!}{\prod_{j=1}^K y_j!} \left[\frac{1-\omega}{K}\right]^{m-y_{k'}^{(1)}} \left[\frac{1-\omega}{K} + \omega\right]^{y_{k'}^{(1)}} \pi_{k'}^{(0)}} && (24)\\
&= \frac{\left[\frac{1-\omega}{K}\right]^m \left(1 + \frac{\omega K}{1-\omega}\right)^{y_k^{(1)}} \pi_k^{(0)}}{\left[\frac{1-\omega}{K}\right]^m \sum_{k'=1}^K \left(1 + \frac{\omega K}{1-\omega}\right)^{y_{k'}^{(1)}} \pi_{k'}^{(0)}} && (25)\\
&= \frac{\pi'^{y_k^{(1)}} \pi_k^{(0)}}{\sum_{k'=1}^K \pi'^{y_{k'}^{(1)}} \pi_{k'}^{(0)}}, && (26)\\
&= \operatorname{softmax}\big(\log \boldsymbol{\pi}^{(0)} + \mathbf{y}^{(1)} \log \pi'\big)_k. && (27)
\end{aligned}$$

Thus, $\boldsymbol{\pi}^{(1)} = \operatorname{softmax}\big(\log \boldsymbol{\pi}^{(0)} + \mathbf{y}^{(1)} \log \pi'\big)$ matching the formula as $\sum_{i=1}^1 \mathbf{y}^{(i)} = \mathbf{y}^{(1)}$.

Inductive step. Assume the statement holds for some $N \geq 1$:

$$\pi_k^{(N)} = \operatorname{softmax}\Big(\log \boldsymbol{\pi}^{(0)} + \Big[\textstyle\sum_{i=1}^N \mathbf{y}^{(i)}\Big] \log \pi'\Big)_k.$$

After receiving $\mathbf{y}^{(N+1)}$ we update:

$$\pi_k^{(N+1)} = \frac{(\pi')^{y_k^{(N+1)}} \pi_k^{(N)}}{\sum_j (\pi')^{y_j^{(N+1)}} \pi_j^{(N)}}. \tag{28}$$

We insert the inductive hypothesis for $\pi_k^{(N)}$:

$$\pi_k^{(N+1)} = \frac{(\pi')^{y_k^{(N+1)}} \pi_k^{(N)}}{\sum_j (\pi')^{y_j^{(N+1)}} \pi_j^{(N)}} \tag{29}$$

$$= \frac{(\pi')^{y_k^{(N+1)}} \dfrac{\exp\big(\log \pi_k^{(0)} + \log \pi' \sum_{i=1}^N y_k^{(i)}\big)}{\sum_\ell \exp\big(\log \pi_\ell^{(0)} + \log \pi' \sum_{i=1}^N y_\ell^{(i)}\big)}}{\sum_j (\pi')^{y_j^{(N+1)}} \dfrac{\exp\big(\log \pi_j^{(0)} + \log \pi' \sum_{i=1}^N y_j^{(i)}\big)}{\sum_\ell \exp\big(\log \pi_\ell^{(0)} + \log \pi' \sum_{i=1}^N y_\ell^{(i)}\big)}} \tag{30}$$

$$= \frac{\exp\big(\log \pi_k^{(0)} + \log \pi' \big[\sum_{i=1}^N y_k^{(i)} + y_k^{(N+1)}\big]\big)}{\sum_j \exp\big(\log \pi_j^{(0)} + \log \pi' \big[\sum_{i=1}^N y_j^{(i)} + y_j^{(N+1)}\big]\big)} \tag{31}$$

$$= \frac{\exp\big(\log \pi_k^{(0)} + \log \pi' \sum_{i=1}^{N+1} y_k^{(i)}\big)}{\sum_j \exp\big(\log \pi_j^{(0)} + \log \pi' \sum_{i=1}^{N+1} y_j^{(i)}\big)}. \tag{32}$$

Because $\sum_{i=1}^N y_k^{(i)} + y_k^{(N+1)} = \sum_{i=1}^{N+1} y_k^{(i)}$, the numerator and denominator are exactly the softmax with the sum taken to $N+1$. Hence

$$\pi_k^{(N+1)} = \operatorname{softmax}\Big(\log \boldsymbol{\pi}^{(0)} + \Big[\textstyle\sum_{i=1}^{N+1} \mathbf{y}^{(i)}\Big] \log \pi'\Big)_k, \tag{33}$$

Thus, $\boldsymbol{\pi}^{(N+1)} = \operatorname{softmax}\Big(\log \boldsymbol{\pi}^{(0)} + \Big[\sum_{i=1}^{N+1} \mathbf{y}^{(i)}\Big] \log \pi'\Big)$ completing the induction. $\square$

Theorem A.2. *Fix $K \geq 2$ and $\omega \in (0, 1)$. Let $x \in \{1, \ldots, K\}$ have prior $\boldsymbol{\pi}_0 \in \Delta_{K-1}$. At each time step $t \in \mathbb{N}$ an observation $\mathbf{y}^{(t)} \in \mathbb{N}^K$ with $\sum_k y_k^{(t)} = m$ is drawn from*

$$p(\mathbf{y}^{(t)} \mid x = k, \omega) \;=\; \frac{m!}{\prod_j y_j^{(t)}!} \Big(\tfrac{1-\omega}{K}\Big)^{m - y_k^{(t)}} \Big(\tfrac{1-\omega}{K} + \omega\Big)^{y_k^{(t)}}.$$

Define $\pi' := 1 + \dfrac{\omega K}{1-\omega}$ and $\Delta\alpha_t := \alpha_t - \alpha_{t-1} = m\omega^2$.

Then the following posterior approximations hold for $m \to \infty$:

1. ***Single–step update.** Given $\boldsymbol{\pi}_{t-1}$, $\boldsymbol{\pi}_t$ can be approximated using a Gaussian random vector:*

$$\boldsymbol{\pi}_t \approx \operatorname{softmax}\big(\log \boldsymbol{\pi}_{t-1} + \mathbf{z}_t\big), \qquad \mathbf{z}_t \sim \mathcal{N}\big(\Delta\alpha_t K \mathbf{e}_x, \Delta\alpha_t K \mathbf{I}\big). \tag{34}$$

2. ***Aggregated update.** $\boldsymbol{\pi}_t$ can be approximated using a Gaussian random vector directly:*

$$\boldsymbol{\pi}_t \approx \operatorname{softmax}(\mathbf{z}_t),\; \mathbf{z}_t \sim \mathcal{N}(\alpha_t K \mathbf{e}_x, \alpha_t K \mathbf{I}). \tag{15}$$

Proof. **(i) Single step.** Conditioned on x, the vector $\mathbf{y}^{(t)}$ is multinomial with parameters m and probabilities

$$\boldsymbol{\theta} = \omega\, \mathbf{e}_x + (1-\omega)\, \tfrac{1}{K}\mathbf{1}. \tag{35}$$

The Central Limit Theorem yields:

$$\mathbf{y}^{(t)} \xrightarrow[m\to\infty]{d} \mathcal{N}\big(m\omega\mathbf{e}_x + (1-\omega)\tfrac{1}{K}\mathbf{1}, m\,\operatorname{diag}(\boldsymbol{\theta}) - \boldsymbol{\theta}\boldsymbol{\theta}^\top\big). \tag{36}$$

By applying a mean-field approximation $\operatorname{diag}(\boldsymbol{\theta}) - \boldsymbol{\theta}\boldsymbol{\theta}^\top \approx \frac{1}{K}\mathbf{I}$ and noting that $\log \pi' \approx \omega K$ since $\omega \to 0$, we obtain:

$$\mathbf{y}^{(t)} \log \pi' \xrightarrow[m\to\infty]{d} \mathcal{N}\big(m\omega^2 K\mathbf{e}_x + \omega(1-\omega)\mathbf{1}, m\omega^2 K\mathbf{I}\big). \tag{37}$$

Since the softmax operation is shift-invariant, we can drop the constant $\omega(1-\omega)\mathbf{1}$ and define $\mathbf{z}_t \sim \mathcal{N}\big(m\omega^2 K\mathbf{e}_x, m\omega^2 K\mathbf{I}\big)$. Plugged into the update, we obtain $\boldsymbol{\pi}_t = \operatorname{softmax}(\log \boldsymbol{\pi}_{t-1} + \mathbf{z}_t)$ matching Eq. (14).

(ii) Aggregation. The vectors $\mathbf{z}_1, \ldots, \mathbf{z}_t$ are conditionally i.i.d. Gaussians; their sum is Gaussian with mean $\sum_{s=1}^t \Delta\alpha_t K\mathbf{e}_x = \alpha_t K\mathbf{e}_x$ and covariance $\sum_{s=1}^t \Delta\alpha_t K\mathbf{I} = \alpha_t K\mathbf{I}$. Because a constant vector can be subtracted inside the softmax, the factor $\log \boldsymbol{\pi}_0$ drops out, yielding $\boldsymbol{\pi}_t = \operatorname{softmax}(\mathbf{z}_t)$ with the stated distribution. □

A.1 Differences to BFNs.

While there is a different theoretical perspective between TreeGen and BFNs, both models build on the same Bayesian update. The key differences mostly occur in the sampling and training procedure. TreeGen performs the following update during sampling:

$$\hat{\boldsymbol{\pi}} = f_\theta(\boldsymbol{\pi}_{t-1}, t-1) \tag{38}$$

$$\mathbf{z}_t \sim \mathcal{N}\big(\alpha_t K\hat{\boldsymbol{\pi}}, \alpha_t K\mathbf{I}\big) \tag{39}$$

$$\boldsymbol{\pi}_t = \operatorname{softmax}(\mathbf{z}_t). \tag{40}$$

In contrast, BFNs perform:

$$\hat{\boldsymbol{\pi}} = f_\theta(\boldsymbol{\pi}_{t-1}, t-1) \tag{41}$$

$$\mathbf{z}_t \sim \mathcal{N}\big(\tfrac{\mathrm{d}\alpha_t}{\mathrm{d}t} K\hat{\boldsymbol{\pi}}, \tfrac{\mathrm{d}\alpha_t}{\mathrm{d}t} K\mathbf{I}\big) \tag{42}$$

$$\boldsymbol{\pi}_t = \operatorname{softmax}(\boldsymbol{\pi}_{t-1} + \mathbf{z}_t). \tag{43}$$

Furthermore, BFNs optimize their framework using the following objective:

$$\mathcal{L}(\theta) = \mathbb{E}_{x\sim\mathcal{D}, t\sim\mathcal{U}(0,1), \boldsymbol{\pi}_t\sim p_t(\boldsymbol{\pi}_t|\mathbf{x})} \left[\frac{\mathrm{d}\alpha_t}{2\mathrm{d}t} \|f_\theta(\boldsymbol{\pi}_t, t) - e_x\|_2^2\right], \tag{44}$$

while TreeGen use the loss presented in Sec. 3.

B Experiment Details

B.1 Hyperparameters

We provide an overview of the training and model hyperparameters in Tab. 3.

Table 3: Hyperparameters of TreeGen.

	Training				Sampling	Graph-Transformer			Upscaler		Prediction Head
	LR	Epochs	Grad. Clip	EMA	Steps	Layers	Dim (h)	Heads	Node Layers	Edge Layers	Layers
Value	10^{-4}	50	0.5	0.9999	1000	4	64	2	1	3	2

All experiments are conducted on A100 GPUs.

B.2 Datasets

We simulate five jet-shower datasets using the GINKGO generator [12]. Three contain QCD jets (QCD-S, QCD-M, QCD-L), and two describe W-boson jets (W-S, W-M). All sets share a common decay rate λ and differ only in the shower cut-off $\Delta_{\text{cut}} \in \{4.0^2,\ 1.1^2,\ 0.6^2\}$, which controls the tree sizes: up to 19 nodes for S, 59 for M, and 99 for L. Each dataset contains 10^5 binary hierarchies, split into 98,000 training examples and 1,000 each for validation and test. Fig. 8 plots the leaf-count distributions of the three QCD samples, illustrating how the cut-off controls the final hierarchy size. Inside every hierarchy, the nodes, i.e., an energy-momentum vector specifies particles:

$$\boldsymbol{p}^{\mu} = \big(E,\ p_x,\ p_y,\ p_z\big), \tag{45}$$

which contains the energy E and momentum (p_x, p_y, p_z). In our setting, we only observe the leaves and infer the hierarchy, i.e., the structure of internal nodes.

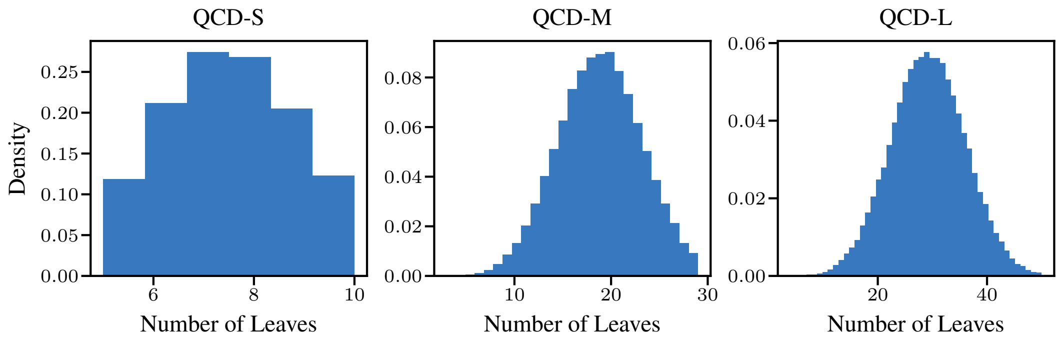

Figure 8: Histogram of the number of leaves for the three different QCD datasets.

In our setup, the tree corresponds to a splitting process. A parent node splits into its children. The root corresponds to the initial particle, while the leaves represent the observed particles. We aim to reconstruct the splitting process, i.e., find the edges of the tree by inferring the parent–child edges given the leaves.

B.3 Architecture

The input to our neural network is a probabilistic hierarchy with $n + n'$ nodes, representing leaves and internal nodes, i.e., $\mathcal{T} \in [0,1]^{(n+n')\times(n+n')}$. Our architecture consists of three components: (*i*) the feature generation (discussed in App. B.4) , (*ii*) a graph transformer, and (*iii*) a prediction head.

Graph Transformer. Given h-dimensional node and edge features, denoted as $\boldsymbol{X} \in \mathbb{R}^{(n+n')\times h}$ and $\boldsymbol{E} \in \mathbb{R}^{m\times h}$, respectively, we iteratively update node features $\boldsymbol{X}^{(l)}$ at layer l given $\boldsymbol{X}^{(l-1)}$, $\boldsymbol{E}$, and the edges of the hierarchy as adjacency matrix $\mathcal{A} \in \{0,1\}^{(n+n')\times(n+n')}$. We use the graph transformer proposed by Shi et al. [38] as our backbone with four layers, two attention heads, and a hidden dimension of 64 (Tab. 3).

Prediction head. Our goal is to predict parent probabilities, i.e., edge probabilities from the node representations of the graph-transformer. Therefore, we apply a prediction head to each child-parent pair $(\mathrm{v}_i, \mathrm{z}_i)$ to obtain a logit for the corresponding edge and apply a softmax over all outgoing edges of the child.

The prediction head concatenates the latent representations of the child and the parent together with the corresponding edge features. These are then passed through a small MLP to obtain the logits as depicted in Fig. 9.

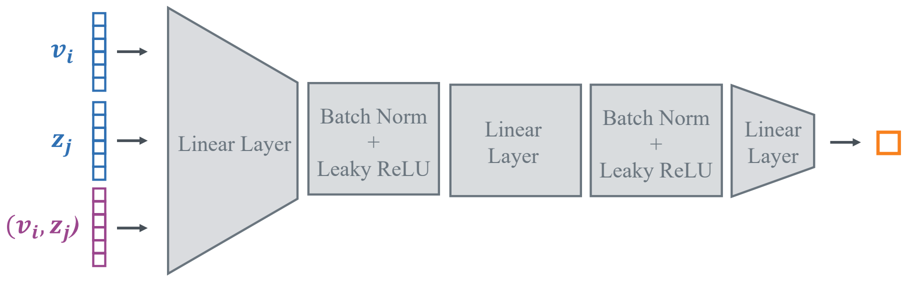

Figure 9: **Prediction head.** The prediction head processes the representations of child-parent pairs $(\mathrm{v}_i, \mathrm{z}_j)$, together with their corresponding edge features, and predicts single logit.

B.4 Feature Generation

To model probabilistic hierarchies effectively, we extract a diverse set of features. We first introduce features encoding structural and uncertainty-related information such as node type, entropy, and ancestor probabilities (App. B.4.1). We then present physically-inspired features, which capture domain-specific properties like momentum, rapidity, and invariant mass (App. B.4.2). Finally, we project raw features into the hidden space used by the network (App. B.4.3).

B.4.1 Features for Probabilistic Hierarchies

In this section, we present node and edge features that can be derived from probabilistic hierarchies and aid the network in obtaining global features. We use the equations and sampling procedure from Zügner et al. [48].

Node Type. If nodes have children, they are categorized as internal nodes; otherwise, as leaves. We represent this with a binary feature. Furthermore, we introduce a binary feature identifying the root, as it is the only node without a parent.

Node Entropy. We model each node's parent assignment as a categorical distribution over its candidate parents and derive two features: (i) the number of candidate parents and (ii) a normalized entropy quantifying uncertainty. Specifically, we compute:

$$\mathcal{H}(\mathrm{v}_i) = -\frac{1}{\log(n')} \sum_{j=1}^{n'} \boldsymbol{A}_{ij} \log \boldsymbol{A}_{ij}, \tag{46}$$

$$\mathcal{H}(\mathrm{z}_i) = -\frac{1}{\log\big(n' - (i+1)\big)} \sum_{j=i+1}^{n'} \boldsymbol{B}_{ij} \log \boldsymbol{B}_{ij}. \tag{47}$$

The logarithmic normalizers match the number of candidate parents in each case, scaling the entropy to $[0, 1]$.

Expected Children. For each internal node z_k, we include the expected number of children under the tree sampling procedure $(\hat{\boldsymbol{A}}, \hat{\boldsymbol{B}}) \sim p_{\boldsymbol{A},\boldsymbol{B}}$ as a feature. Under $p_{\boldsymbol{A},\boldsymbol{B}}$, this equals the total probability that z_k is chosen as the parent of each leaf and each earlier internal node $j < k$:

$$\mathbb{E}\left[n_{\text{child}}(\mathrm{z}_k)\right] = \sum_{i=1}^{n} p(\mathrm{z}_k \mid \mathrm{v}_i) + \sum_{j=1}^{k-1} p(\mathrm{z}_k \mid \mathrm{z}_j) \tag{48}$$

$$= \sum_{i=1}^{n} \boldsymbol{A}_{ik} + \sum_{j=1}^{k-1} \boldsymbol{B}_{jk}, \tag{49}$$

where A_i and B_j denote the parent of leaf v_i and internal node z_j, respectively. The equalities follow from the linearity of expectation and $\mathbb{E}[\mathbb{I}[X = k]] = \Pr(X = k)$.

Sibling Probability. We encode the sibling relation, i.e., whether two nodes share the same parent, by its probability under the tree-sampling procedure as edge features. For leaves v_i and v_j, we compute the probability by:

$$p\left(\mathrm{v}_i \text{ and } \mathrm{v}_j \text{ are siblings}\right) = \sum_{k=1}^{n'} p(\mathrm{z}_k \mid \mathrm{v}_i, \mathrm{z}_k \mid \mathrm{v}_j) \tag{50}$$

$$= \sum_{k=1}^{n'} p(\mathrm{z}_k \mid \mathrm{v}_i)\, p(\mathrm{z}_k \mid \mathrm{v}_j) \tag{51}$$

$$= \sum_{k=1}^{n'} \boldsymbol{A}_{ik} \boldsymbol{A}_{jk}, \tag{52}$$

where we used the independence of parent draws in the sampling procedure. For internal nodes, we compute this quantity using $\boldsymbol{B}$, summing only over feasible parents.

Ancestor Features. We use two ancestor-based features. (i) *Ancestor probability* as an edge feature for an internal node z_k and a node v_i, let $P^{\text{anc}}_{ik} := p(\mathrm{z}_k \in \operatorname{anc}(\mathrm{v}_i))$ denote the probability—under the tree-sampling procedure—that z_k is an ancestor of v_i. (ii) *Expected number of ancestors* as a node feature, which equals the node's expected depth.

For a leaf v_i, we compute the expected number of ancestors as:

$$\mathbb{E}[n_{\text{anc}}(\mathrm{v}_i)] = \mathbb{E}\left[\sum_{k=1}^{n'} \mathbb{I}[\mathrm{z}_k \in \operatorname{anc}(\mathrm{v}_i)]\right] \tag{53}$$

$$= \sum_{k=1}^{n'} p(\mathrm{z}_k \in \operatorname{anc}(\mathrm{v}_i)) \tag{54}$$

$$= \sum_{k=1}^{n'} P^{\text{anc}}_{ik}. \tag{55}$$

The computation for internal nodes follows analogously, using the matrix $\tilde{P}^{\text{anc}}$.

For a pair of nodes, we also compute the (expected) number of *shared* ancestors as a similarity measure. As we cannot derive an exact expression due to the dependence between the ancestor probabilities $p(\mathrm{z}_k \in \operatorname{anc}(\mathrm{v}_i))$ and $p(\mathrm{z}_k \in \operatorname{anc}(\mathrm{v}_j))$, we use an independence approximation:

$$\mathbb{E}[n_{\text{anc}}(\mathrm{v}_i, \mathrm{v}_j)] \;\approx\; \sum_{k=1}^{n'} P^{\text{anc}}_{ik}\, P^{\text{anc}}_{jk}. \tag{56}$$

The computation of P^{anc} and $\tilde{P}^{\text{anc}}$ follows Zügner et al. [48].

Hierarchy size. As the hierarchies can vary in size within the datasets, we include the hierarchy size, i.e., the number of nodes, as a feature.

Time embeddings. In addition to the probabilistic hierarchies and their derived features, we include the time $t \in [0, 1]$ as input to the network. We use a 10-dimensional sinusoidal positional encoding as done in the transformer architecture [44]. We concatenate these embeddings to the node features.

B.4.2 Physically Inspired Features

In addition to the task-agnostic features described above, we include physically inspired features tailored to jet clustering. Each node in the hierarchy corresponds to a particle and is described by its four-momentum vector

$$\boldsymbol{p}^{\mu} = (E, p_x, p_y, p_z), \tag{57}$$

which serves as the basis for our physics-derived features. The momentum $\vec{p} = (p_x, p_y, p_z)$ is defined in three spatial directions: the z-axis is aligned with the beam (beamline), and the plane spanned by the two axes orthogonal to z is the transverse plane.

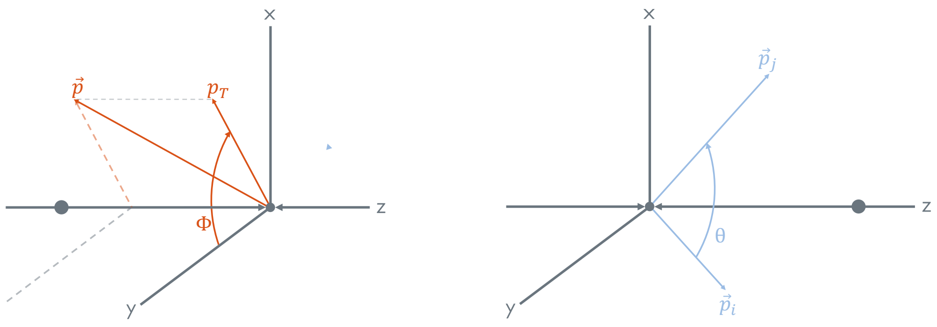

Figure 10: Illustration of the transverse momentum p_T and the azimuth ϕ (*left*), and the angle θ between the momentum vectors of two particles (*right*).

Transverse Momentum. The transverse plane is crucial for analyzing the dynamics of particle interactions and scatterings. A key quantity in this context is the transverse momentum:

$$p_T := \sqrt{p_x^2 + p_y^2}, \tag{58}$$

which we include as a node feature.

Angular Features. Following the anti-k_T algorithm, we compute the azimuth ϕ and the rapidity y, which define the pairwise distance measure used by the algorithm. The azimuth ϕ is measured in the transverse plane and is computed as:

$$\phi := \arctan\left(\frac{p_x}{p_y}\right). \tag{59}$$

The rapidity y is related to the angle of a particle relative to the beamline. It is especially useful in high-energy physics as it remains approximately invariant under boosts along the beam axis:

$$y := \frac{1}{2}\log\left(\frac{E + p_z}{E - p_z}\right). \tag{60}$$

We include ϕ and y as node features and, analogously to the anti-k_T algorithm, use their differences as edge features:

$$\Delta\phi = \phi_i - \phi_j \qquad \text{and} \qquad \Delta y = y_i - y_j \tag{61}$$

As an additional edge feature, we use the angle θ, which accounts for all momentum components and is given by:

$$\theta = \arccos\left(\frac{\vec{p}_i^T \vec{p}_j}{\|\vec{p}_i\|_2 \|\vec{p}_j\|_2}\right), \tag{62}$$

where $\vec{p} = (p_x, p_y, p_z)$ is the momentum vector of a particle. We illustrate the angles ϕ and θ in Fig. 10.

Invariant Mass. Finally, we use the squared invariant mass, which represents the intrinsic mass of a particle independent of its motion or reference frame:

$$\Delta = E^2 - (p_x^2 + p_y^2 + p_z^2). \tag{63}$$

This property plays a crucial role in the splits within our hierarchies. As discussed in Section B.2, the invariant mass of a parent particle must be greater than the sum of the invariant masses of its children. Hence, for any internal node z_k with children v_i and z_j:

$$\sqrt{\Delta_{\mathrm{z}_k}} \geq \sqrt{\Delta_{\mathrm{v}_i}} + \sqrt{\Delta_{\mathrm{z}_j}}. \tag{64}$$

In the probabilistic setting, we relax this condition to

$$\sqrt{\Delta_{\mathrm{z}_k}} \geq \sum_{i=1}^{n} \boldsymbol{A}_{ik} \sqrt{\Delta_{\mathrm{v}_i}} + \sum_{j=1}^{k-1} \boldsymbol{B}_{jk} \sqrt{\Delta_{\mathrm{z}_j}}. \tag{65}$$

We use the difference between the invariant mass of the parent node and the weighted sum of the invariant masses of its children as a node feature. Additionally, we include binary variables whether Δ_{z_k} exceeds the cut thresholds and whether it's larger than 0.

We also derive edge features from this constraint. For each pair of nodes, we compute the energy-momentum vector of their potential parent and calculate the difference between the invariant mass of this potential parent and the sum of the invariant masses of the two children. This edge feature effectively quantifies the plausibility of the nodes being siblings.

B.4.3 Feature Upscaling

To align inputs with the hidden size h and stabilize training, we normalize node features with batch normalization, apply a linear layer, and then a LeakyReLU. Because the backbone does not update edge features, we process them using three successive blocks. The upscaling block is shown in Fig. 11. These serve as input to our backbone (see App. B.3).

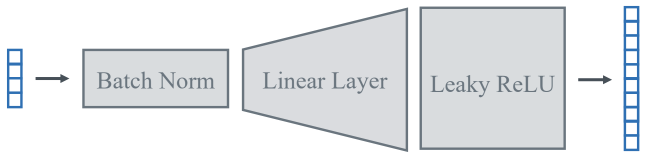

Figure 11: **Feature Upscaler.** The feature upscaler processes the input features and maps them to the hidden dimension h.

B.5 Baselines

In the following, we give a short description of the baselines. Both generative models operate on probabilistic hierarchies, just like TreeGen. We keep architecture, features, training, and sampling parameters consistent.

Bayesian Flow Networks (BFNs). The most related baselines are standard BFNs. We discuss details and differences to our model in App. A. For the implementation, we keep it as similar as possible to TreeGen. While we use our proposed entropy scheduler as explained in Sec. 3, we perform training and sampling as described by Graves et al. [19].

CatFlow. CatFlow [16] is a flow-matching model that evolves samples on the probability simplex by integrating an ODE whose vector field is parametrized by a neural network. Training uses a cross-entropy loss to predict the ground-truth hierarchy from noisy ones, similar to TreeGen. Two key differences remain: *(i)* CatFlow's trajectories are not constrained to stay on the simplex during integration. We use a Gaussian prior with mean and standard deviation of 0.25, clipped at 10^{-4} to enable the computation of all features, and *(ii)* the generative process is deterministic once the prior sample is fixed.

anti-k_t jet clustering algorithm. The anti-k_t is a well-established algorithm [7]. It iteratively merges the two entities, i.e., particles or pseudojets, with the smallest pairwise distances d_{ij}. The distances are computed based on the transverse momentum, azimuth angle, and rapidity (see App. B.4).

B.6 Metrics

We report two complementary, physics-aware metrics.

Valid Hierarchy Percentage (Valid Fraction). A hierarchy is *valid* if it satisfies three conditions:

- **(i)** it is a binary decay tree
- **(ii)** at every internal node the invariant mass exceeds those of the sum of the children
- **(iii)** the squared invariant mass of each internal particle exceeds the dataset-specific cut-off.

For every generated hierarchy, we check these conditions and return the percentage that are valid.

Ratio of Log-Likelihoods (LLH Fraction). Physical plausibility does not guarantee that samples follow the data distribution. Leveraging the Ginkgo simulator, we compute the log-likelihood of each generated hierarchy (ℓ_{gen}) and of its ground-truth counterpart (ℓ_{true}). We report the average ratio $\ell_{\text{true}}/\ell_{\text{gen}}$ over the test set. A value close to one indicates that the generative model aligns with the target distribution.

C Additional Results

C.1 Feature ablation

In the following, we ablate core features discussed in App. B.4 on QCD-S. We start with a base model that neither uses features from the ancestor nor physical properties. The results are shown in Tab. 4.

Table 4: Ablation of ancestor and physically inspired features.

Model	Valid Frac. (↑)	LLH Frac.
Base model	0.563 ± 0.004	0.937 ± 0.002
+ Ancestor Features	0.564 ± 0.001	0.939 ± 0.001
+ 4-Momentum + Angular Features	0.645 ± 0.021	0.982 ± 0.001
+ Invariant Mass	0.997 ± 0.001	1.003 ± 0.002

We observe that the base model only provides 56.3% of valid trees. While including the ancestor features only provides marginal improvements, the physically inspired features yield major improvements.

C.2 Comparison to clustering algorithms.

In Tab. 5, we compare TreeGen to the CA [15, 46], k_t [17], and anti-k_t [7] jet clustering algorithm. As we observe, TreeGen consistently outperforms the traditional clustering algorithms in terms of valid hierarchies. In terms of likelihood, the k_t algorithm achieves slightly higher scores.

Table 5: Comparison between clustering algorithms and TreeGen. Best scores in **bold**.

Dataset	CA		k_t		anti-k_t		TreeGen	
	Valid (↑)	LLH	Valid (↑)	LLH	Valid (↑)	LLH	Valid (↑)	LLH
QCD-S	0.416	0.989	0.302	**1.029**	0.840	0.873	**0.997** ±0.001	1.003 ±0.002
QCD-M	0.088	0.987	0.050	**1.050**	0.552	0.752	**0.977** ±0.010	0.994 ±0.002
QCD-L	0.025	0.978	0.008	**1.065**	0.440	0.636	**0.943** ±0.016	0.975 ±0.001

NeurIPS Paper Checklist

1. **Claims**

   Question: Do the main claims made in the abstract and introduction accurately reflect the paper's contributions and scope?

   Answer: [Yes]

   Justification: We propose TreeGen in Sec. 3 and demonstrate its performance empirically on the jet clustering task in Sec. 4

   Guidelines:

   - The answer NA means that the abstract and introduction do not include the claims made in the paper.
   - The abstract and/or introduction should clearly state the claims made, including the contributions made in the paper and important assumptions and limitations. A No or NA answer to this question will not be perceived well by the reviewers.
   - The claims made should match theoretical and experimental results, and reflect how much the results can be expected to generalize to other settings.
   - It is fine to include aspirational goals as motivation as long as it is clear that these goals are not attained by the paper.

2. **Limitations**

   Question: Does the paper discuss the limitations of the work performed by the authors?

   Answer: [Yes]

   Justification: We include a separate limitations paragraph in Sec. 6 and discuss potential future work. All assumptions are stated when applicable.

   Guidelines:

   - The answer NA means that the paper has no limitation while the answer No means that the paper has limitations, but those are not discussed in the paper.
   - The authors are encouraged to create a separate "Limitations" section in their paper.
   - The paper should point out any strong assumptions and how robust the results are to violations of these assumptions (e.g., independence assumptions, noiseless settings, model well-specification, asymptotic approximations only holding locally). The authors should reflect on how these assumptions might be violated in practice and what the implications would be.
   - The authors should reflect on the scope of the claims made, e.g., if the approach was only tested on a few datasets or with a few runs. In general, empirical results often depend on implicit assumptions, which should be articulated.
   - The authors should reflect on the factors that influence the performance of the approach. For example, a facial recognition algorithm may perform poorly when image resolution is low or images are taken in low lighting. Or a speech-to-text system might not be used reliably to provide closed captions for online lectures because it fails to handle technical jargon.
   - The authors should discuss the computational efficiency of the proposed algorithms and how they scale with dataset size.
   - If applicable, the authors should discuss possible limitations of their approach to address problems of privacy and fairness.
   - While the authors might fear that complete honesty about limitations might be used by reviewers as grounds for rejection, a worse outcome might be that reviewers discover limitations that aren't acknowledged in the paper. The authors should use their best judgment and recognize that individual actions in favor of transparency play an important role in developing norms that preserve the integrity of the community. Reviewers will be specifically instructed to not penalize honesty concerning limitations.

3. **Theory assumptions and proofs**

   Question: For each theoretical result, does the paper provide the full set of assumptions and a complete (and correct) proof?

Answer: [Yes]

Justification: We discuss theoretical properties and assumptions in App. A.

Guidelines:

- The answer NA means that the paper does not include theoretical results.
- All the theorems, formulas, and proofs in the paper should be numbered and cross-referenced.
- All assumptions should be clearly stated or referenced in the statement of any theorems.
- The proofs can either appear in the main paper or the supplemental material, but if they appear in the supplemental material, the authors are encouraged to provide a short proof sketch to provide intuition.
- Inversely, any informal proof provided in the core of the paper should be complemented by formal proofs provided in appendix or supplemental material.
- Theorems and Lemmas that the proof relies upon should be properly referenced.

4. **Experimental result reproducibility**

   Question: Does the paper fully disclose all the information needed to reproduce the main experimental results of the paper to the extent that it affects the main claims and/or conclusions of the paper (regardless of whether the code and data are provided or not)?

   Answer: [Yes]

   Justification: We describe our algorithm in Sec. 3 and the experimental setup in Sec. 4. Furthermore, we specify our architecture and features in App. B.3 and App. B.4. All hyperparameters are listed in App. B.1

   Guidelines:

   - The answer NA means that the paper does not include experiments.
   - If the paper includes experiments, a No answer to this question will not be perceived well by the reviewers: Making the paper reproducible is important, regardless of whether the code and data are provided or not.
   - If the contribution is a dataset and/or model, the authors should describe the steps taken to make their results reproducible or verifiable.
   - Depending on the contribution, reproducibility can be accomplished in various ways. For example, if the contribution is a novel architecture, describing the architecture fully might suffice, or if the contribution is a specific model and empirical evaluation, it may be necessary to either make it possible for others to replicate the model with the same dataset, or provide access to the model. In general. releasing code and data is often one good way to accomplish this, but reproducibility can also be provided via detailed instructions for how to replicate the results, access to a hosted model (e.g., in the case of a large language model), releasing of a model checkpoint, or other means that are appropriate to the research performed.
   - While NeurIPS does not require releasing code, the conference does require all submissions to provide some reasonable avenue for reproducibility, which may depend on the nature of the contribution. For example
     (a) If the contribution is primarily a new algorithm, the paper should make it clear how to reproduce that algorithm.
     (b) If the contribution is primarily a new model architecture, the paper should describe the architecture clearly and fully.
     (c) If the contribution is a new model (e.g., a large language model), then there should either be a way to access this model for reproducing the results or a way to reproduce the model (e.g., with an open-source dataset or instructions for how to construct the dataset).
     (d) We recognize that reproducibility may be tricky in some cases, in which case authors are welcome to describe the particular way they provide for reproducibility. In the case of closed-source models, it may be that access to the model is limited in some way (e.g., to registered users), but it should be possible for other researchers to have some path to reproducing or verifying the results.

5. **Open access to data and code**

Question: Does the paper provide open access to the data and code, with sufficient instructions to faithfully reproduce the main experimental results, as described in supplemental material?

Answer: [Yes]

Justification: The code is available on the project page and contains instructions to reproduce the main experimental results.

Guidelines:

- The answer NA means that paper does not include experiments requiring code.
- Please see the NeurIPS code and data submission guidelines (`https://nips.cc/public/guides/CodeSubmissionPolicy`) for more details.
- While we encourage the release of code and data, we understand that this might not be possible, so "No" is an acceptable answer. Papers cannot be rejected simply for not including code, unless this is central to the contribution (e.g., for a new open-source benchmark).
- The instructions should contain the exact command and environment needed to run to reproduce the results. See the NeurIPS code and data submission guidelines (`https://nips.cc/public/guides/CodeSubmissionPolicy`) for more details.
- The authors should provide instructions on data access and preparation, including how to access the raw data, preprocessed data, intermediate data, and generated data, etc.
- The authors should provide scripts to reproduce all experimental results for the new proposed method and baselines. If only a subset of experiments are reproducible, they should state which ones are omitted from the script and why.
- At submission time, to preserve anonymity, the authors should release anonymized versions (if applicable).
- Providing as much information as possible in supplemental material (appended to the paper) is recommended, but including URLs to data and code is permitted.

6. **Experimental setting/details**

   Question: Does the paper specify all the training and test details (e.g., data splits, hyperparameters, how they were chosen, type of optimizer, etc.) necessary to understand the results?

   Answer: [Yes]

   Justification: All experimental details are specified in Sec. 4 and App. B.1.

   Guidelines:

   - The answer NA means that the paper does not include experiments.
   - The experimental setting should be presented in the core of the paper to a level of detail that is necessary to appreciate the results and make sense of them.
   - The full details can be provided either with the code, in appendix, or as supplemental material.

7. **Experiment statistical significance**

   Question: Does the paper report error bars suitably and correctly defined or other appropriate information about the statistical significance of the experiments?

   Answer: [Yes]

   Justification: Our results include standard deviations computed over four seeds.

   Guidelines:

   - The answer NA means that the paper does not include experiments.
   - The authors should answer "Yes" if the results are accompanied by error bars, confidence intervals, or statistical significance tests, at least for the experiments that support the main claims of the paper.
   - The factors of variability that the error bars are capturing should be clearly stated (for example, train/test split, initialization, random drawing of some parameter, or overall run with given experimental conditions).

- The method for calculating the error bars should be explained (closed form formula, call to a library function, bootstrap, etc.)
- The assumptions made should be given (e.g., Normally distributed errors).
- It should be clear whether the error bar is the standard deviation or the standard error of the mean.
- It is OK to report 1-sigma error bars, but one should state it. The authors should preferably report a 2-sigma error bar than state that they have a 96% CI, if the hypothesis of Normality of errors is not verified.
- For asymmetric distributions, the authors should be careful not to show in tables or figures symmetric error bars that would yield results that are out of range (e.g. negative error rates).
- If error bars are reported in tables or plots, The authors should explain in the text how they were calculated and reference the corresponding figures or tables in the text.

8. **Experiments compute resources**

   Question: For each experiment, does the paper provide sufficient information on the computer resources (type of compute workers, memory, time of execution) needed to reproduce the experiments?

   Answer: [Yes]

   Justification: We specify the compute resources in App. B.

   Guidelines:

   - The answer NA means that the paper does not include experiments.
   - The paper should indicate the type of compute workers CPU or GPU, internal cluster, or cloud provider, including relevant memory and storage.
   - The paper should provide the amount of compute required for each of the individual experimental runs as well as estimate the total compute.
   - The paper should disclose whether the full research project required more compute than the experiments reported in the paper (e.g., preliminary or failed experiments that didn't make it into the paper).

9. **Code of ethics**

   Question: Does the research conducted in the paper conform, in every respect, with the NeurIPS Code of Ethics `https://neurips.cc/public/EthicsGuidelines`?

   Answer: [Yes]

   Justification: We read the code of ethics and our paper conform with it.

   Guidelines:

   - The answer NA means that the authors have not reviewed the NeurIPS Code of Ethics.
   - If the authors answer No, they should explain the special circumstances that require a deviation from the Code of Ethics.
   - The authors should make sure to preserve anonymity (e.g., if there is a special consideration due to laws or regulations in their jurisdiction).

10. **Broader impacts**

    Question: Does the paper discuss both potential positive societal impacts and negative societal impacts of the work performed?

    Answer: [NA]

    Justification: This paper proposes a generative model for hierarchies empirically evaluated on the jet clustering task that does not have direct societal impact.

    Guidelines:

    - The answer NA means that there is no societal impact of the work performed.
    - If the authors answer NA or No, they should explain why their work has no societal impact or why the paper does not address societal impact.

- Examples of negative societal impacts include potential malicious or unintended uses (e.g., disinformation, generating fake profiles, surveillance), fairness considerations (e.g., deployment of technologies that could make decisions that unfairly impact specific groups), privacy considerations, and security considerations.
- The conference expects that many papers will be foundational research and not tied to particular applications, let alone deployments. However, if there is a direct path to any negative applications, the authors should point it out. For example, it is legitimate to point out that an improvement in the quality of generative models could be used to generate deepfakes for disinformation. On the other hand, it is not needed to point out that a generic algorithm for optimizing neural networks could enable people to train models that generate Deepfakes faster.
- The authors should consider possible harms that could arise when the technology is being used as intended and functioning correctly, harms that could arise when the technology is being used as intended but gives incorrect results, and harms following from (intentional or unintentional) misuse of the technology.
- If there are negative societal impacts, the authors could also discuss possible mitigation strategies (e.g., gated release of models, providing defenses in addition to attacks, mechanisms for monitoring misuse, mechanisms to monitor how a system learns from feedback over time, improving the efficiency and accessibility of ML).

11. **Safeguards**

    Question: Does the paper describe safeguards that have been put in place for responsible release of data or models that have a high risk for misuse (e.g., pretrained language models, image generators, or scraped datasets)?

    Answer: [NA]

    Justification: This paper does not pose risks for misuse.

    Guidelines:

    - The answer NA means that the paper poses no such risks.
    - Released models that have a high risk for misuse or dual-use should be released with necessary safeguards to allow for controlled use of the model, for example by requiring that users adhere to usage guidelines or restrictions to access the model or implementing safety filters.
    - Datasets that have been scraped from the Internet could pose safety risks. The authors should describe how they avoided releasing unsafe images.
    - We recognize that providing effective safeguards is challenging, and many papers do not require this, but we encourage authors to take this into account and make a best faith effort.

12. **Licenses for existing assets**

    Question: Are the creators or original owners of assets (e.g., code, data, models), used in the paper, properly credited and are the license and terms of use explicitly mentioned and properly respected?

    Answer: [Yes]

    Justification: We cite the Ginkgo simulator.

    Guidelines:

    - The answer NA means that the paper does not use existing assets.
    - The authors should cite the original paper that produced the code package or dataset.
    - The authors should state which version of the asset is used and, if possible, include a URL.
    - The name of the license (e.g., CC-BY 4.0) should be included for each asset.
    - For scraped data from a particular source (e.g., website), the copyright and terms of service of that source should be provided.
    - If assets are released, the license, copyright information, and terms of use in the package should be provided. For popular datasets, `paperswithcode.com/datasets` has curated licenses for some datasets. Their licensing guide can help determine the license of a dataset.

- For existing datasets that are re-packaged, both the original license and the license of the derived asset (if it has changed) should be provided.
- If this information is not available online, the authors are encouraged to reach out to the asset's creators.

13. **New assets**

    Question: Are new assets introduced in the paper well documented and is the documentation provided alongside the assets?

    Answer: [NA]

    Justification: We do not introduce new assets.

    Guidelines:

    - The answer NA means that the paper does not release new assets.
    - Researchers should communicate the details of the dataset/code/model as part of their submissions via structured templates. This includes details about training, license, limitations, etc.
    - The paper should discuss whether and how consent was obtained from people whose asset is used.
    - At submission time, remember to anonymize your assets (if applicable). You can either create an anonymized URL or include an anonymized zip file.

14. **Crowdsourcing and research with human subjects**

    Question: For crowdsourcing experiments and research with human subjects, does the paper include the full text of instructions given to participants and screenshots, if applicable, as well as details about compensation (if any)?

    Answer: [NA]

    Justification: Our paper does not include research with human subjects or crowdsourcing.

    Guidelines:

    - The answer NA means that the paper does not involve crowdsourcing nor research with human subjects.
    - Including this information in the supplemental material is fine, but if the main contribution of the paper involves human subjects, then as much detail as possible should be included in the main paper.
    - According to the NeurIPS Code of Ethics, workers involved in data collection, curation, or other labor should be paid at least the minimum wage in the country of the data collector.

15. **Institutional review board (IRB) approvals or equivalent for research with human subjects**

    Question: Does the paper describe potential risks incurred by study participants, whether such risks were disclosed to the subjects, and whether Institutional Review Board (IRB) approvals (or an equivalent approval/review based on the requirements of your country or institution) were obtained?

    Answer: [NA]

    Justification: Our paper does not include research with human subjects or crowdsourcing.

    Guidelines:

    - The answer NA means that the paper does not involve crowdsourcing nor research with human subjects.
    - Depending on the country in which research is conducted, IRB approval (or equivalent) may be required for any human subjects research. If you obtained IRB approval, you should clearly state this in the paper.
    - We recognize that the procedures for this may vary significantly between institutions and locations, and we expect authors to adhere to the NeurIPS Code of Ethics and the guidelines for their institution.
    - For initial submissions, do not include any information that would break anonymity (if applicable), such as the institution conducting the review.

16. **Declaration of LLM usage**

    Question: Does the paper describe the usage of LLMs if it is an important, original, or non-standard component of the core methods in this research? Note that if the LLM is used only for writing, editing, or formatting purposes and does not impact the core methodology, scientific rigorousness, or originality of the research, declaration is not required.

    Answer: [NA]

    Justification: Our method does not involve LLMs.

    Guidelines:

    - The answer NA means that the core method development in this research does not involve LLMs as any important, original, or non-standard components.
    - Please refer to our LLM policy (`https://neurips.cc/Conferences/2025/LLM`) for what should or should not be described.